Dijoux *et al. Microbiome* (2025) 13:110
https://doi.org/10.1186/s40168-025-02098-7

Microbiome

RESEARCH

Open Access

Plant nickel-exclusion versus hyperaccumulation: a microbial perspective

Julie Dijoux[1*], Sarah Gigante[1], Gael Lecellier[1], Linda Guentas[1] and Valérie Burtet-Sarramegna[1*]

Abstract

Background In New Caledonia, nearly 2000 plant species grow on ultramafic substrates, which contain prominent levels of heavy metals and are deficient in essential plant nutrients. To colonize these habitats, such plants, known as metallophytes, have developed various adaptive behaviors towards metals (exclusion, tolerance, or hyperaccumulation). Ultramafic substrates also host many unique microorganisms, which are adapted to metallic environments and capable of boosting plant growth while assisting plants in acquiring essential micronutrients. Hence, plant-microbiota interactions play a key role in adapting to environmental stress. Here, we hypothesised that microbial associations in the different aboveground and underground compartments of metallophytes could be associated to their metal hyperaccumulation or exclusion phenotypes. This hypothesis was tested using a systematic comparative metabarcoding approach on the different compartments of two New Caledonian metallophytes belonging to the same genus and living in sympatry on ultramafic substrates: *Psychotria gabriellae*, a nickel-hyperaccumulator (Ni-HA), and *Psychotria semperflorens*, the related non-accumulator (nA) species.

Results The study of the diversity and specificity of fungal amplicon sequence variants (ASVs) reveals a structuring of fungal communities at both the plant phenotype and compartment levels. In contrast, the structure of bacterial communities was primarily shaped by the belowground compartments. Additionally, we observed a lower diversity in the bacterial communities of the aboveground compartments of each species. For each plant species, we highlighted a distinct global microbial signature (biomarkers), as well as compartment-specific microbial associations.

Conclusion To our knowledge, this study is the first to systematically compare the microbiomes associated with different compartments of New Caledonian metallophyte species growing on the same substrate and under identical environmental conditions but exhibiting different adaptive phenotypes. Our results reveal distinct microbial biomarkers between the Ni-hyperaccumulator and non-accumulator *Psychotria* species. Most of the highlighted biomarkers are abundant in various plants under metal stress and may contribute to improving the phytoextraction or phytostabilization processes. They are also known to tolerate heavy metals and enhance metal stress tolerance in plants. The present findings highlight that the microbial perspective is essential for better understanding the mechanisms of hyperaccumulation and exclusion at the whole-plant level.

Keywords Bacteria, Fungi, Hyperaccumulation, Metabarcoding, Metallophytes, Microbiota, Nickel, *Psychotria* sp., Ultramafic Substrates

*Correspondence:
Julie Dijoux
juu.dijoux@gmail.com
Valérie Burtet-Sarramegna
valerie.sarramegna@unc.nc

Background

At low or moderate concentrations, certain metallic trace elements (MTEs) are essential plant nutrients. However, at high concentrations, they can become toxic and disrupt basic plant metabolic processes [1, 2]. Some plants, known as metallophytes, can grow in metal-rich environments without exhibiting deleterious symptoms through adaptive mechanisms [3]. These include restricting metal entry into cells (excluders) or modulating stress (accumulators and hyperaccumulators) by sequestering MTEs in different organs [4]. Metal uptake restriction, the first line of defence, involves root exudates that alter rhizospheric pH or chelate MTEs, thus immobilising them in the rhizosphere or aiding their translocation and detoxification in plant tissues. Under metal stress, transporters such as zinc/iron-regulated transporter-like proteins (ZIP) and heavy-metal P-type ATPases (HMA) can be overexpressed [2], playing roles in metal homeostasis and contributing to the hyperaccumulation phenotype.

The adaptation of plants to metals also depends on the plant-associated microbiota [5, 6]. The rhizosphere of hyperaccumulators may act as a valuable reservoir of specialised metal-tolerant microorganisms [7]. Indeed, metal-tolerant bacteria and fungi can bioaccumulate metals inside their cells, adsorb them onto their cell surfaces, or bind them to extracellular polysaccharides, affecting the bioavailability of MTEs in soil and transforming them into less toxic forms through intra- or extracellular processes [8–11]. Additionally, bacteria and fungi can promote plant growth under stress by stimulating root development, improving nutrient uptake, enhancing soil fertility, regulating pathogens, and boosting immunity [12, 13]. These plant-beneficial microorganisms (PBMs) can also increase plant resistance, tolerance, and MTE accumulation [7, 14]. In association, PBMs can have a synergistic effect [15] and may be more effective in promoting plant growth and removing metallic/organic pollutants [16]. To understand how beneficial microbial associations help plants colonise metal-rich substrates and modulate metal stress, studying the entire plant microbiota is essential. Advances in next-generation sequencing have facilitated studies on the rhizosphere, endosphere [17, 18], and seeds of hyperaccumulators, in which a common microbial core has been highlighted among certain hyperaccumulator families [19].

New Caledonia is a major reservoir of Ni-hyperaccumulators (Ni-HA), thriving on ultramafic substrates rich in heavy metals but deficient in essential nutrients, with an imbalanced Ca/Mg ratio [20, 21]. These extreme edaphic conditions foster high diversity and endemism, offering a unique opportunity to study Ni hyperaccumulation phenotypes. Previous studies have identified ligands and transporters involved in Ni hyperaccumulation, including chelation by citric, maleic, salicylic, fumaric, malonic, ketogluconic, and galacturonic acids, as well as nicotianamine in hyperaccumulator leaves [22]. Additionally, IRON-Regulated 1/Ferroportin transporters have been shown to play a key role in Ni uptake in species like *Psychotria gabriellae* (formerly known as *P. douarrei*), a hypernickelophore (> 1% Ni in leaves) [23–25]. Despite these findings, no systematic investigation has assessed the role of New Caledonian metallophyte microbiota in hyperaccumulation or exclusion. Culture-dependent studies, however, suggest that microorganisms from pioneer plants in ultramafic soils can enhance plant adaptation to metal stress, with some strains exhibiting MTE sorption capacity [26–28].

In this study, we investigated the microbiota of two endemic New Caledonian metallophytes to better understand microbial roles in nickel hyperaccumulation and exclusion on ultramafic substrates. We selected two sympatric *Psychotria* species with contrasting Ni-adaptive strategies: the hyperaccumulator *P. gabriellae* (Pg, Ni-HA) and the non-accumulator *P. semperflorens* (Ps, nA). Using metabarcoding, we characterised their bacterial and fungal communities across six compartments: leaves, seeds, pulps, roots, rhizospheric soil, and bulk soil. Our aim was to determine (a) whether microbial communities are structured by plant compartment and/or phenotype, and (b) whether Pg (Ni-HA) and Ps (nA) exhibit distinct microbial signatures (that might be involved in their differing phenotypes). We identified compartment-specific microbial biomarkers through an integrated approach combining linear discriminant and graph network analyses (Fig. 1).

Methods

Sampling and sample conditioning

According to the Environment Code of the South Province of New Caledonia (collect authorisation number: 4597–2022), sampling was conducted at an ultramafic massif called "Mont Koghi" (Fig. 2), where the two species grow in sympatry, located in the southern part of the main island, "Grande Terre" (21.31 °S, 165.30 °E).

The sampling campaign began at the end of the wet season and continued into the dry season, with collections conducted between March and September 2022. Sampling was extended to align with plant fruiting periods, ensuring sufficient material while minimising the impact on individuals. We selected 13 specimens of *Psychotria gabriellae* (Pg, Ni-HA) and 9 specimens of *Psychotria semperflorens* (Ps, nA). For each plant individual (specimen), we collected leaves, fruits, thin roots, and rhizospheric soil. Additionally, we collected 10 cores of bulk soil (Bs) from the surrounding area of the study site

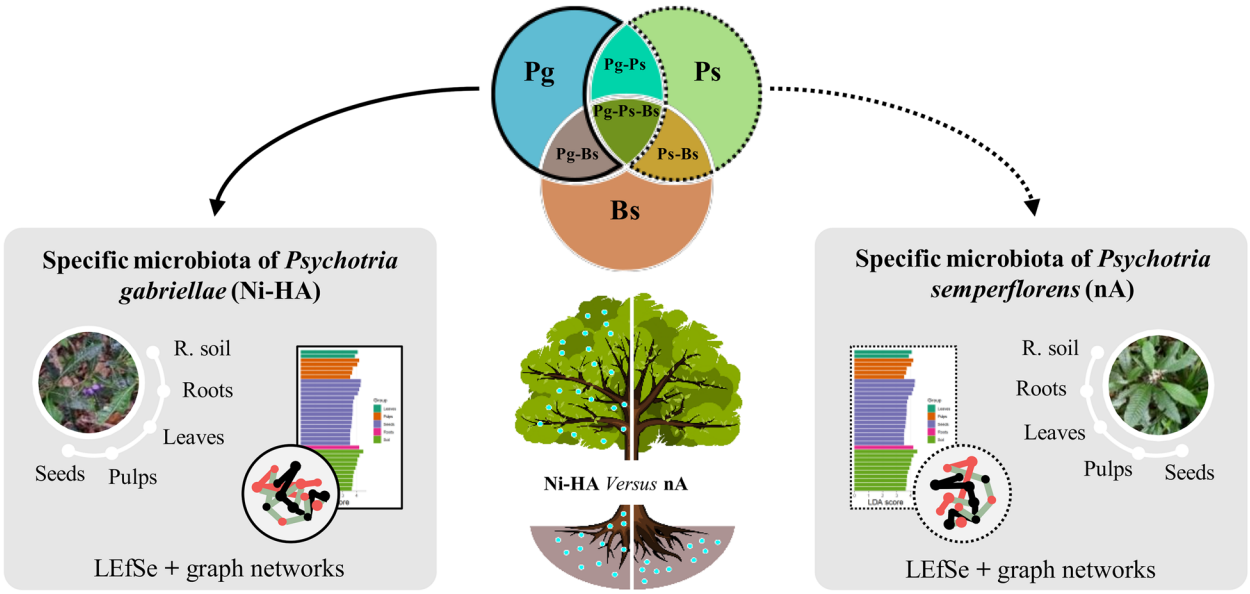

Fig. 1 Overview of the integrated approach applied to the specific microbiotas of *Psychotria gabriellae* (Pg, Ni-HA) and *Psychotria semperflorens* (Ps, nA). Bs: bulk soil; R. soil: rhizospheric soil

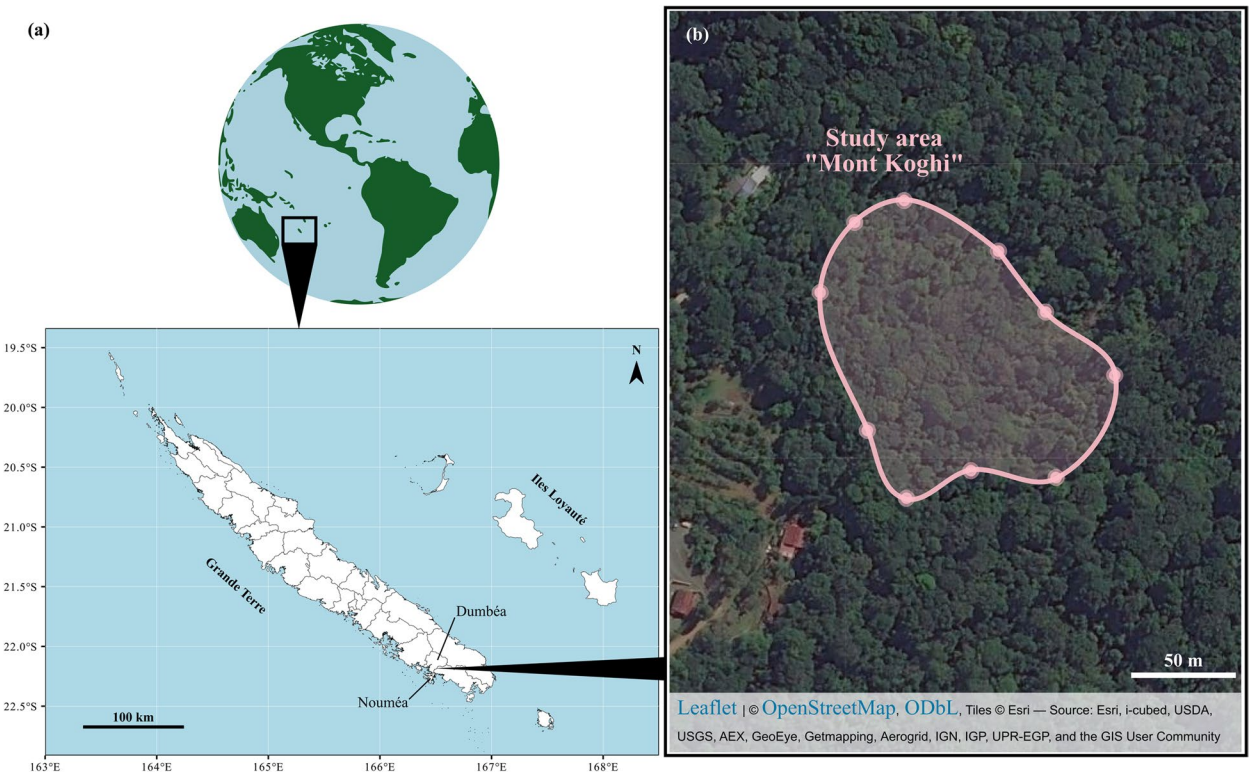

Fig. 2 Location of New Caledonia and its main island, "Grande Terre" (**a**), and the study area (**b**). The New Caledonia map was produced with *ggplot2* (v3.5.1) [29], using terrestrial administrative boundaries from https://georep-dtsi-sgt.opendata.arcgis.com/. The study area map was generated with *leaflet* (v2.2.2) [30]

at a depth of 0–20 cm, matching the sampling depth for roots and rhizospheric soil. This bulk soil, not directly associated with the plants, was used to compare with rhizospheric soil and identify microorganisms potentially recruited by each plant.

Aboveground compartments—leaves, pulps, and seeds—were thoroughly disinfected to study only the endophytic microbial communities. For disinfecting leaves, the following protocol was employed: the leaves were first washed three times with sterile water. They were then shaken for 10 s in 95% ethanol, followed by three additional washes with sterile water. Next, the leaves were shaken for 1–2 min in a 2% calcium hypochlorite solution, then washed three times with sterile water. Following this, the leaves were shaken for 10 min in a 2% T chloramine solution with a few drops of Tween20, then washed three more times with sterile water. Finally, the leaves were shaken for 10 min in an antibiotic solution containing 0.02% streptomycin sulfate and 0.01% gentamicin sulfate [31, 32]. Lastly, leaves were dried with sterile absorbent paper. Using the protocol of Villegente [33], the fruits were first disinfected, followed by the recovery of the pulp (tissue surrounding the seed itself within the fruit), and then the seeds were disinfected [33]. For the roots, since both endophytic and surface-associated microorganisms were targeted, only three washes with sterile water were performed. After disinfection and washing, these compartments were lyophilised and stored at −80 °C until required for DNA extraction.

Rhizospheric and bulk soils were dried at 60 °C for 3 days. They were then sieved through 2 mm, 1.25 mm, and 0.5 mm mesh to remove rocks and plant residues, and ground to homogenise the substrate. The samples were subsequently stored at −80 °C.

DNA extraction

For each compartment and species, a composite sample was created with multiple technical replicates (15 for roots, leaves, and soils compartments; 10 for pulps and seeds compartments). This method allows us to study the plant microbiota at the population level and minimises fine-scale spatial heterogeneity in soil microorganisms [17, 34]. All eDNA was extracted using a CTAB protocol except for soil samples (1 g), which were extracted with the E.Z.N.A.® Soil DNA Kit according to the manufacturer's instructions. The CTAB protocol used is an adaptation of the RNA extraction method described by Salzman et al. [35]. The detailed protocol is described in Additional file 1. The quality of the extracted DNA was validated by agarose gel electrophoresis, while the purity and concentration of the DNA were assessed using a NanoDrop 2000™ spectrophotometer (Thermo Scientific, Waltham, MA, USA). All DNA samples were stored at −20 °C before shipment to the sequencing company.

Library preparation and sequencing

Macrogen Inc. (Seoul, South Korea) performed the amplification and sequencing libraries using Illumina MiSeq SBS (Sequencing By Synthesis) technology. The V3–V4 region of the 16S rRNA gene was amplified for bacterial communities using primers Bakt_341F (5′-CCT ACGGGNGGCWGCAG- 3′) and 805R (5′-GACTAC HVGGGTATCTAATCC- 3′) [36], while the ITS region was amplified for fungal communities using primers ITS-1F (5′-CTTGGTCATTTAGAGGAAGTAA- 3′) and ITS-2R (5′-GCTGCGTTCTTCATCGATGC- 3′) [37].

Bioinformatic pipeline

Pre-processing

A total of 8,658,812 and 10,110,995 reads were obtained for the bacterial and fungal libraries, respectively. The average number of reads per sample was 52,798 for the bacterial library and 61,652 for the fungal library. We first assessed the quality of each read from Macrogen Inc. using the *FastQC* package (v0.12.1) [38] and generated a report with *MULTIQC* (v1.0.dev0) [39] in a *Python* (v2.7) [40] environment. To remove all adapters and primers, we used the *cutadapt* package (v4.4) [41] with the following parameters: a minimum length of 20 nucleotides was retained (-m 20), and untrimmed reads were discarded.

DADA2 workflow

To filter, remove chimeras, and perform taxonomic assignment, we used the DADA2 workflow (v1.26.0) [42, 43]. We filtered and trimmed the reads with the following parameters: truncation based on quality scores of 10 (truncQ = 10) and length-based truncation with truncLen = c(227,205) for the bacterial library and truncLen = c(170,170) for the fungal library. We set a maximum expected error rate of 2 (maxEE = 2). Chimeras were removed using the pooled method, and taxonomic assignment was performed with the formatted SILVA database version 138.1 [44] for the bacterial library and the updated UNITE all eukaryote version 9.0 database [45] for the fungal library. To validate the quality of the filtered sequences, we conducted a second quality control report using *FastQC* and *MULTIQC*.

Correcting, filtering, and normalising data

Abundance tables of amplicon sequence variants (ASVs) from the DADA2 workflow were corrected using negative extraction controls. A total of 3933 and 161,010 sequences were removed from the bacterial and fungal abundance tables, respectively. Taxa not affiliated with Bacteria and Fungi were removed from the bacterial

(1,226,768 sequences) and fungal (1,517,936 sequences) ASV tables, using the *microeco* R package (v1.2.0) [46]. The abundance tables were then normalised to counts per million (CPM). All these steps and subsequent statistical analyses were performed using R (v4.2.0) [47] with RStudio software [48]. Overall, 147 out of 152 samples were sequenced, with 131 passing bioinformatics processing for the 16S library. For the ITS library, 146 out of 152 samples were sequenced, with 145 passing bioinformatics processing.

Statistical analysis

Alpha diversity

Shannon and Inverse Simpson indices were calculated on the corrected, filtered, and normalised abundance tables using the *vegan* R package (v2.6–4) [49]. The mean and standard deviation for each index were computed using the *aggregate* function from the *stats* R package. As the data did not follow a normal distribution (p-value < 0.05; computed using the *shapiro.test* function from the *stats* R package), a Wilcoxon test was performed using the *wilcox.test* function from the *stats* package, with p-value adjustment applied using the fdr method. Tukey's letters were then determined using the *rcompanion* package (v2.4.34) [50].

Relative abundances were calculated and visualised using the *microeco* package. To provide an overview of the data, bacterial and fungal profiles at the class level were displayed for each compartment and each species using stacked bar plots. Note that the analysis of relative abundance was restricted to taxa with an abundance of 0.1% or greater. As with alpha diversity, the data did not follow a normal distribution, so a Wilcoxon test was performed with the fdr method for p-value adjustment (see Additional file 2).

Beta diversity

The distance matrix of beta diversity was generated using the *vegan* package with the Morisita method [51]. The optimal number of clusters (k) was determined using the hierarchical merging method, and ascending hierarchical clustering was then performed with the ward.D2 method using the *hclust* function from the *stats* R package.

ASV distributions

Truth tables were calculated using the *venn* package (v1.12) [52], and Venn diagrams were created using Inkscape software [53]. Subsequently, the list of ASVs for each logical relationship between Pg (Ni-HA), Ps (nA), and Bs (bulk soil) was determined using the *Reduce* and *setdiff* functions in R. These lists of ASV distributions allowed us to focus on ASVs that were exclusively present in each species ("Pg" and "Ps" subsets) and those specifically recruited by each species ("Pg-Bs" and "Ps-Bs" subsets). To simplify subsequent analyses, we combined the "exclusive ASVs" and "specifically recruited ASVs" for each species, resulting in two specific subsets of ASVs corresponding to the specific microbiotas of Pg (Ni-HA) and Ps (nA) (Fig. 1). Using the same method, we then determined the distribution of these specific ASVs across the different compartments for each plant species.

Linear discriminant analysis effect size

Linear discriminant analysis (LDA) effect sizes (LEfSe) were calculated using the *microeco* package. This method enabled us to characterise the differences between compartments in the specific microbiotas of Pg (Ni-HA) and Ps (nA). It identified discriminative features (biomarkers) that were statistically significant across compartments. To pinpoint specific microbial signatures for each species and each compartment (biomarkers), we conducted LEfSe analysis at the genus level on the two specific microbiotas (Fig. 1), applying a p-value threshold of 0.05 (see Additional file 3).

Co-occurrence networks

To complete the analysis, we aimed to identify specific associations between microorganisms within each compartment of the specific microbiotas of Pg (Ni-HA) and Ps (nA) (Fig. 1). We conducted Spearman correlation tests for each compartment of our two specific subsets using the *psych* package (v2.3.9) [54]. We then selected only the significant positive correlations (R > 0.6 and p-value < 0.05) and created graph networks for each compartment using the *igraph* package (v1.5.1) [55]. To assess network stability and resilience, we calculated connectance, average degree, modularity, degree centralisation, and betweenness centrality [56]. Structural parameters for each graph network are available in Additional file 4. In these graph networks, vertices/nodes represent the ASVs, and links/edges denote the significant positive correlations between microbial ASVs (Additional file 4). By integrating the graph networks with the LEfSe results, we identified specific biomarkers that co-occur across the compartments of each species [57].

Results

Alpha diversity

A total of 3908, 3550, and 3805 bacterial ASVs were associated with Bs, Pg (Ni-HA), and Ps (nA), respectively. On average, the number of distinct ASVs per species and compartment ranged from 1 to around 1000. Belowground compartments (roots and rhizospheric soil) consistently exhibited a significantly higher abundance of ASVs (585–977 observed ASVs) compared to aboveground compartments (leaves, pulps, and seeds),

Table 1 Alpha diversity indices for bacterial communities

Species and compartment[a]	*N*[b]	Observed	Shannon	InvSimpson[c]
Pg (Ni-HA) seeds	3	1 ± 1 bf	0.23 ± 0.4 h	1.33 ± 0.58 h
Ps (nA) seeds	8	7 ± 2 c	1.31 ± 0.34 g	3.08 ± 1.63 g
Pg (Ni-HA) pulps	10	8 ± 2 c	1.79 ± 0.26 e	4.88 ± 1.16 e
Ps (nA) pulps	8	20 ± 3 g	2.52 ± 0.19 f	9.53 ± 2.35 f
Pg (Ni-HA) leaves	13	2 ± 1 b	0.59 ± 0.53 h	2.06 ± 1.36 h
Ps (nA) leaves	10	1 ± 0 f	0.2 ± 0.33 h	1.28 ± 0.45 h
Pg (Ni-HA) roots	16	623 ± 205 d	5.58 ± 0.12 a	87.43 ± 8.22 b
Ps (nA) roots	15	585 ± 64 d	5.46 ± 0.08 d	71.22 ± 7.37 d
Pg (Ni-HA) soil	16	784 ± 143 e	5.12 ± 0.11 b	27.19 ± 2.33 c
Ps (nA) soil	16	878 ± 140 ae	5.23 ± 0.11 i	31.68 ± 3.12 i
Bulk soil	16	977 ± 264 a	6.34 ± 0.33 c	255.23 ± 42.31 a

Observed, Shannon, and InvSimpson values are presented as mean ± standard deviation and Tukey's letter

[a] Pg = *Psychotria gabriellae* (Ni-HA) and Ps = *Psychotria semperflorens* (nA)

[b] *N* = number of samples

[c] InvSimpson = Inverse Simpson

which had between 1 and 20 observed ASVs, regardless of the species (Table 1, Fig. 3).

This trend was consistent across all alpha diversity indices, with Shannon (H) indices ranging from 0.23 to 2.52 in aboveground compartments and from 5.12 to 6.34 in belowground compartments. Similarly, Inverse Simpson indices ranged from 1.28 to 9.53 in aboveground compartments and from 27.19 to 255.23 in belowground compartments. Significant differences in diversity between species (e.g., pulps and seeds) were observed. Furthermore, when comparing the diversity of bulk soil to rhizospheric soil, both H and Inverse Simpson indices were significantly lower in rhizospheric soil for each species, as well as in fungal indices.

In the fungal analysis, a total of 2236, 2124, and 2761 ASVs were associated with Bs, Pg (Ni-HA), and Ps (nA), respectively. On average, we observed ranges from 10 to around 600 ASVs per species and compartment. Belowground compartments consistently showed a significantly higher abundance of ASVs (246–577 observed ASVs) compared to aboveground compartments (10–149 observed ASVs) for each species (Table 2, Fig. 4).

This trend did not align with the H and Inverse Simpson indices. Specifically, the leaves compartments exhibited significantly higher diversity than the roots for each species and were even more diverse than the rhizospheric soil in Ps (nA). Inter-species comparisons also revealed significant differences, particularly within the leaves compartment.

Table 2 Alpha diversity indices for fungal communities

Species and compartment[a]	*N*[b]	Observed	Shannon	InvSimpson[c]
Pg (Ni-HA) seeds	9	10 ± 3 g	0.35 ± 0.33 f	1.23 ± 0.33 f
Ps (nA) seeds	8	10 ± 2 g	0.9 ± 0.08 i	1.74 ± 0.1 h
Pg (Ni-HA) pulps	10	58 ± 7 f	1.61 ± 0.16 e	2.67 ± 0.54 e
Ps (nA) pulps	8	49 ± 8 h	1.06 ± 0.09 h	1.47 ± 0.06 g
Pg (Ni-HA) leaves	16	90 ± 12 b	3.42 ± 0.13 b	11.46 ± 1.99 b
Ps (nA) leaves	16	149 ± 23 e	4.31 ± 0.19 d	49.03 ± 12.05 a
Pg (Ni-HA) roots	16	246 ± 30 c	2.23 ± 0.54 c	3.73 ± 1.31 c
Ps (nA) roots	14	308 ± 14 d	3.96 ± 0.12 g	15.03 ± 3.15 d
Pg (Ni-HA) soil	16	327 ± 47 d	3.93 ± 0.17 g	14.24 ± 2.19 d
Ps (nA) soil	16	382 ± 37 i	3.53 ± 0.31 b	7.04 ± 1.6 i
Bulk soil	16	577 ± 88 a	4.96 ± 0.1 a	49.91 ± 6.42 a

Observed, Shannon, and InvSimpson values are presented as mean ± standard deviation and Tukey's letter

[a] Pg = *Psychotria gabriellae* (Ni-HA) and Ps = *Psychotria semperflorens* (nA)

[b] *N* = number of samples

[c] InvSimpson = Inverse Simpson

Beta diversity

As determined by the merge fusion figure, the bacterial communities were structured into 8 clusters (see Additional file 5). In belowground compartments, the bacterial community structure was distinct between roots (k2_B), rhizospheric soil (k1_B), and bulk soil (k3_B). However, these structures appeared to be similar between species. In contrast, for aboveground compartments, the leaves samples from each species were grouped with the seed samples of Pg (Ni-HA) (k6_B, k7_B, and k8_B). Only the pulps compartment of Pg (Ni-HA) (k5_B) and the fruits—both pulps and seeds—of Ps (nA) (k4_B) exhibited distinct bacterial community structures.

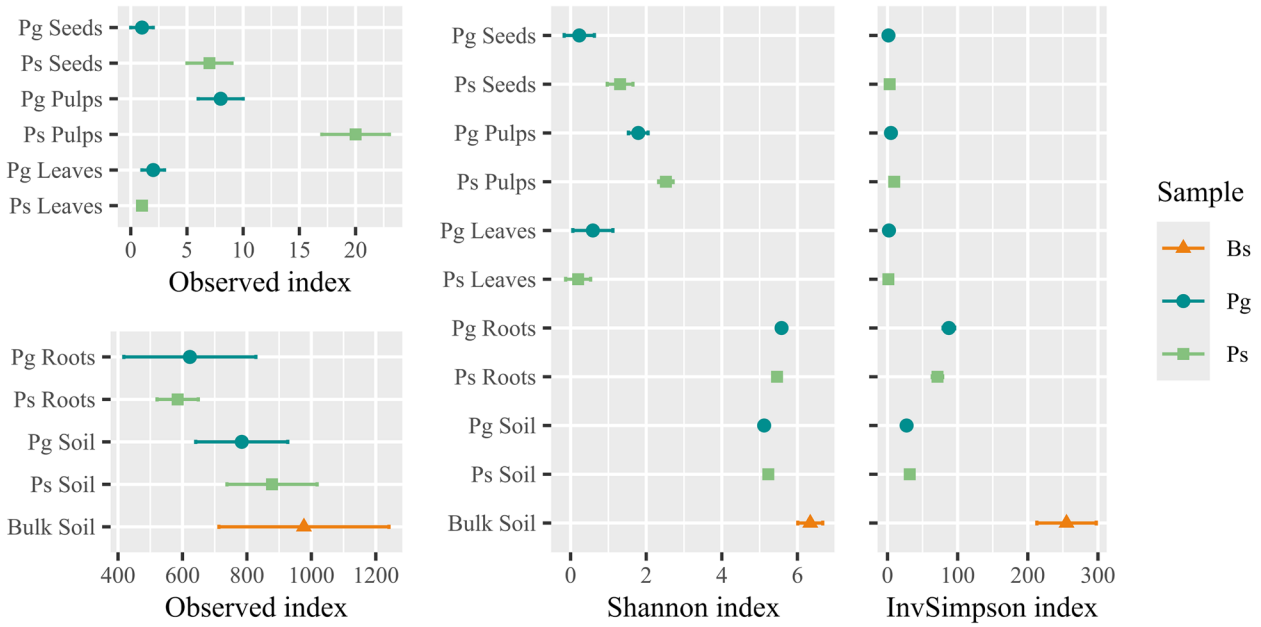

Fig. 3 Cleveland diagram of alpha diversity indices for bacterial communities. (Pg = *Psychotria gabriellae* (Ni-HA), Ps = *Psychotria semperflorens* (nA), and InvSimpson = Inverse Simpson)

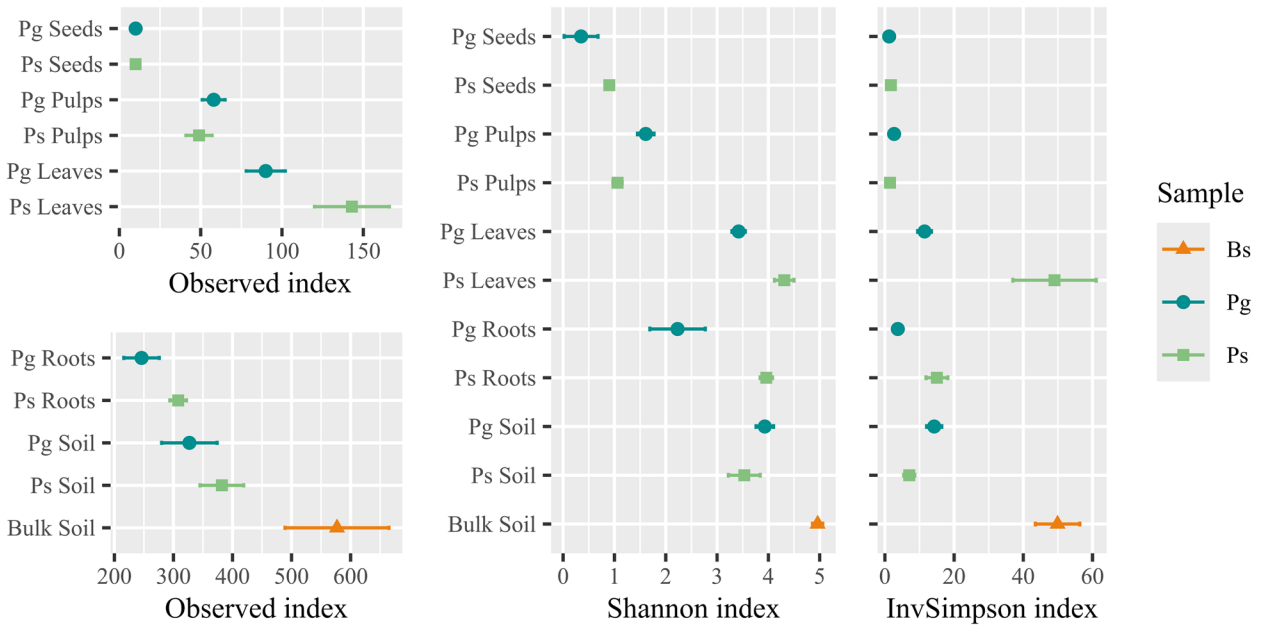

Fig. 4 Cleveland diagram of alpha diversity indices for fungal communities. (Pg = *Psychotria gabriellae* (Ni-HA), Ps = *Psychotria semperflorens* (nA), and InvSimpson = Inverse Simpson)

Concerning fungal communities, the merge fusion figure revealed 10 clusters (see Additional file 5). Unlike bacterial community structures, belowground compartments were distinct between species and compartments: k1_F for Pg (Ni-HA) rhizospheric soil, k2_F for Ps (nA) rhizospheric soil, k3_F for bulk soil, k4_F and k5_F for Pg (Ni-HA) roots, and k6_F for Ps (nA) roots. For aboveground compartments, the clustering differentiated between leaves samples (k7_F for Ps (nA), and k8_F for Pg (Ni-HA)) and fruit samples—both pulps and

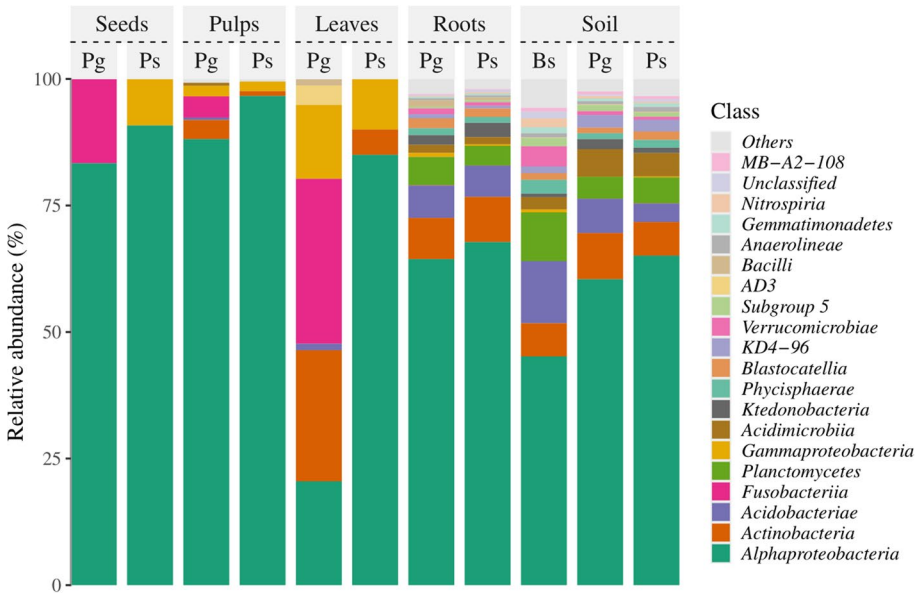

Fig. 5 Relative abundances of the 20 most abundant bacterial taxa at the class level in *Psychotria gabriellae* (Pg, Ni-HA), *Psychotria semperflorens* (Ps, nA) and bulk soil (Bs)

seeds—of each species (k9_F for Pg (Ni-HA) and k10_F for Ps (nA)).

Structure of bacterial communities at class level

A total of 71 classes were identified in the bacterial library. Bulk soil exhibited the highest class diversity, with 40 classes, followed by: Pg (Ni-HA) roots (35 classes) > Ps (nA) rhizospheric soil (32 classes) > Pg (Ni-HA) rhizospheric soil and Ps (nA) roots (28 classes) > Pg (Ni-HA) pulps (8 classes) > Pg (Ni-HA) leaves (7 classes) > Ps (nA) pulps (5 classes) > Ps (nA) leaves (3 classes) > Pg (Ni-HA) and Ps (nA) seeds (2 classes) (Fig. 5).

For most compartments and both species, *Alphaproteobacteria* (20.5–96.6%) was the most abundant taxon, while the second and third most abundant taxa varied depending on the species and the compartment.

Structure of bacterial communities of Psychotria gabriellae (Pg, Ni-HA)

Overall, more classes were observed in belowground compartments compared to aboveground compartments, with a similar distribution between roots and rhizospheric soil compartments (Fig. 5). *Alphaproteobacteria* dominated both compartments (60.4% in rhizospheric soil and 64.4% in roots), followed by taxa such as *Actinobacteria* (8.1% in roots and 9.1% in rhizospheric soil), *Acidobacteriae* (6.4% in roots and 6.8% in rhizospheric soil), *Acidimicrobiia* (1.6% in roots and 5.4% in rhizospheric soil), *Planctomycetes* (4.3% in rhizospheric soil and 5.6% in roots), and *Ktedonobacteria* (1.9% in roots and 2.0% in rhizospheric soil). In addition to shared classes, these compartments also exhibited specific, rare classes. For example, *Dehalococcoidia* (0.1%) was only present in rhizospheric soil, while *Bacteroidia* (0.2%), *Armatimonadia* (0.2%), *Polyangia* (0.1%), *Parcubacteria* (0.1%), *Myxococcia* (0.1%), and *Methylomirabilia* (0.1%) were found exclusively in roots.

In the aboveground compartments, *Alphaproteobacteria* was the most abundant taxon in seeds (83.3%) and pulps (88.1%). However, in leaves, this class was less abundant (20.5%), with the difference being significant only when compared to bulk soil (see Additional file 2). *Fusobacteriia* was also present as an abundant taxon in all aboveground compartments (32.6% in leaves, 16.7% in seeds, and 4.2% in pulps). *Actinobacteria* (25.9% in leaves and 3.8% in pulps), *Gammaproteobacteria* (14.6% in leaves and 2.1% in pulps), and *Acidobacteriae* (1.3% in leaves and 0.5% in pulps) were shared between leaves and pulps. Notably, leaves and pulps each contained unique classes: AD3 (*Chloroflexi* phylum 3.8%) was exclusive to leaves, and *Campylobacteria* (0.5%) was unique to pulps.

In summary, there was a clear distinction between the bacterial community structures of aboveground and belowground compartments in Pg (Ni-HA). Additionally, apart from seeds, few classes were specific to any single compartment in Pg (Ni-HA).

Structure of bacterial communities of Psychotria semperflorens (Ps, nA)

Alphaproteobacteria was the most abundant taxon in each compartment: pulps (96.0%), seeds (90.8%), leaves (85.0%), roots (67.8%), and rhizospheric soil (65.1%) (Fig. 5). *Actinobacteria* and *Gammaproteobacteria* were the only other taxa shared across all compartments. As observed in Pg (Ni-HA), the belowground compartments of Ps (nA) exhibited a more diverse class composition than the aboveground compartments. The composition between roots and rhizospheric soil was similar, with a high abundance of *Alphaproteobacteria*, followed by *Actinobacteria* (8.9% in roots and 6.6% in rhizospheric soil), *Acidobacteriae* (6.2% in roots and 3.4% in rhizospheric soil), and *Planctomycetes* (3.9% in roots and 5.1% in rhizospheric soil). These two compartments also contained specific rare classes: *Armatimonadia* (0.2%) and *Bacteroidia* (0.1%) in roots, and *Thermoleophilia* (0.5%), bacteriap25 (*Myxococcota* phylum 0.2%), *Methylomirabilia* (0.1%), *Dehalococcoidia* (0.1%), JG30-KF-CM66 (*Chloroflexi* phylum 0.1%), and *Limnochordia* (0.1%) in rhizospheric soil.

In the aboveground compartments, each compartment was primarily composed of *Alphaproteobacteria* (90.8% in seeds, 96.6% in pulps, and 85.0% in leaves) and *Gammaproteobacteria* (9.2% in seeds, 1.9% in pulps, and 10.0% in leaves). Notably, pulps contained a specific class: *Deinococci* (0.3%).

In summary, like Pg (Ni-HA), the structure of bacterial communities differed significantly between aboveground and belowground compartments in Ps (nA). Additionally, rhizospheric soil, roots, and leaves also contained unique bacterial classes.

Inter-species comparison at the compartment level

When comparing bacterial classes between plant species within the same compartment, each plant species exhibited specific bacterial classes at the compartment level (Fig. 5). In seeds, *Fusobacteriia* (16.7%) and *Gammaproteobacteria* (9.2%) were specific to Pg (Ni-HA) and Ps (nA), respectively. In pulps, *Fusobacteriia* (4.2%), *Acidimicrobiia* (0.6%), *Acidobacteriae* (0.5%), *Campylobacteria* (0.5%), and *Clostridia* (0.3%) were specific to Pg (Ni-HA), while *Deinococci* (0.3%) and *Saccharimonadia* (0.2%) were specific to Ps (nA). In leaves and roots, only Pg (Ni-HA) exhibited specific classes: *Fusobacteriia* (32.6%), AD3 (*Chloroflexi* phylum 3.8%), and *Bacilli* (1.3%) in leaves, and *Polyangia* (0.1%), *Parcubacteria* (0.1%), *Thermoleophilia* (0.1%), *Myxococcia* (0.1%), bacteriap25 (*Myxococcota* phylum 0.1%), *Methylomirabilia* (0.1%), and *Fusobacteriia* (0.1%) in roots. Finally, only Ps (nA) exhibited specific classes in its rhizospheric soil: *Gammaproteobacteria* (0.2%), *Methylomirabilia* (0.1%), JG30-KF-CM66 (*Chloroflexi* phylum 0.1%), and *Limnochordia* (0.1%).

Structure of fungal communities at class level

Overall, 47 classes were observed in the fungal library. Bulk soil, along with Pg (Ni-HA) rhizospheric soil, exhibited the highest class diversity (18 classes) among compartments and species, followed by: Ps (nA) rhizospheric soil (17 classes) > Ps (nA) leaves (15 classes) > Ps (nA) roots (13 classes) > Pg (Ni-HA) leaves (12 classes) > Pg (Ni-HA) roots (11 classes) > Pg (Ni-HA) and Ps (nA) pulps (9 classes) > Pg (Ni-HA) seeds (8 classes) > Ps (nA) seeds (5 classes) (Fig. 6).

In contrast to bacterial communities, a significant proportion of unclassified fungi at the class level predominantly composed the fruits of Ps (nA), with 74.6% in seeds and 83.7% in pulps. This was also observed in the roots of Ps (nA) (49.1%) and bulk soil (30.3%). The proportion of unclassified fungi remained substantial in other compartments, ranging from 11.3 to 25.3%, except in Pg (Ni-HA) seeds, where it was markedly lower at 0.5%.

Structure of fungal communities of Psychotria gabriellae (Pg, Ni-HA)

The structure of fungal communities varied significantly between compartments (Fig. 6). Although most classes were shared, they were not represented in the same proportions across compartments. Seeds were primarily composed of *Dothideomycetes* (91.9%) and *Agaricomycetes* (6.0%). Pulps consisted of *Dothideomycetes* (59.6%), unclassified fungi (24.2%), *Tremellomycetes* (5.8%), and *Sordariomycetes* (6.5%). Leaves contained *Dothideomycetes* (39.7%), *Sordariomycetes* (38.2%), and unclassified fungi (19.6%). Roots were composed of *Agaricomycetes* (70.6%), unclassified fungi (13.2%), *Leotiomycetes* (6.5%), and *Sordariomycetes* (5.3%). Finally, rhizospheric soil included *Mortierellomycetes* (36.8%), *Agaricomycetes* (28.2%), unclassified fungi (16.0%), and *Sordariomycetes* (8.1%).

Some classes were specific to certain compartments. GS35 (*Ascomycota* phylum 0.4%), *Basidiobolomycetes* (0.3%), *Microbotryomycetes* (0.2%), *Ramicandelaberomycetes* (0.3%), *Tritirachiomycetes* (0.2%), *Pucciniomycetes* (0.1%), and *Atractiellomycetes* (0.1%) were only found in rhizospheric soil, whereas *Geminibasidiomycetes* (0.1%) and *Umbelopsidomycetes* (0.1%) were specific to leaves.

Structure of fungal communities of Psychotria semperflorens (Ps, nA)

Like Pg (Ni-HA), the structure of fungal communities in Ps (nA) varied significantly between compartments (Fig. 6). Although abundant classes were shared, their proportions differed across compartments. Seeds

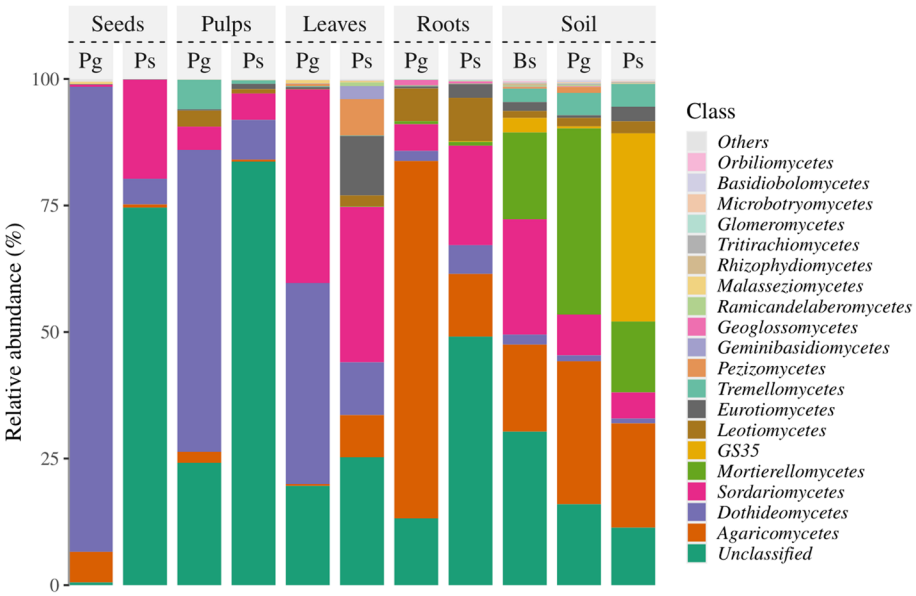

Fig. 6 Relative abundances of the 20 most represented fungal taxa at the class level in *Psychotria gabriellae* (Pg, Ni-HA), *Psychotria semperflorens* (Ps, nA) and bulk soil (Bs)

were primarily composed of unclassified fungi (74.6%), *Sordariomycetes* (19.6%), and *Dothideomycetes* (5.1%). Pulps consisted mainly of unclassified fungi (83.7%), *Dothideomycetes* (7.9%), and *Sordariomycetes* (5.2%). Leaves contained *Sordariomycetes* (30.7%), unclassified fungi (25.3%), *Eurotiomycetes* (11.7%), *Dothideomycetes* (10.4%), *Agaricomycetes* (8.3%), and *Pezizomycetes* (7.2%). Roots were composed of unclassified fungi (49.1%), *Sordariomycetes* (19.7%), *Agaricomycetes* (12.4%), *Leotiomycetes* (8.5%), and *Dothideomycetes* (5.7%). Finally, rhizospheric soil included GS35 (*Ascomycota* phylum 37.2%), *Agaricomycetes* (20.6%), *Mortierellomycetes* (14.0%), unclassified fungi (11.3%), *Sordariomycetes* (5.2%), and *Tremellomycetes* (4.5%).

Each compartment, except for seeds, contained specific classes. *Tritirachiomycetes* (0.2%), *Spizellomycetes* (0.1%), *Microbotryomycetes* (0.1%), *Saccharomycetes* (0.1%), and *Pucciniomycetes* (0.1%) were exclusive to rhizospheric soil. *Geoglossomycetes* (0.4%) and *Glomeromycetes* (0.2%) were specific to roots. In aboveground compartments, *Geminibasidiomycetes* (2.6%), *Umbelopsidomycetes* (0.2%), *Malasseziomycetes* (0.2%), and GS14 (*Chytridiomycota* phylum 0.1%) were unique to leaves, while *Ustilaginomycetes* (0.1%) and *Lecanoromycetes* (0.1%) were specific to pulps.

Inter-species comparison at compartment level

The comparison of fungal community structures between species within the same compartment revealed notable differences between Pg (Ni-HA) and Ps (nA) (Fig. 6). Even within identical compartments, species exhibited significantly distinct community structures (Additional file 2). As discussed in the previous sections, while abundant classes were shared, their proportions differed significantly between species. For instance, *Mortierellomycetes* was the most abundant class in Pg (Ni-HA) rhizospheric soil, whereas GS35 (*Ascomycota* phylum) dominated in Ps (nA) rhizospheric soil.

In aboveground compartments, the fungal composition of seeds differed markedly between species. Seeds of Pg (Ni-HA) were primarily composed of *Dothideomycetes* (91.9%, $p < 0.001$), while seeds of Ps (nA) consisted mainly of unclassified fungi (74.6%) and *Sordariomycetes* (19.6%, $p < 0.01$). In this compartment, only Pg (Ni-HA) contained specific classes compared to Ps (nA): *Malasseziomycetes* (0.5%), *Wallemiomycetes* (0.4%), and *Cystobasidiomycetes* (0.1%). In pulps, *Dothideomycetes*, *Tremellomycetes*, and *Leotiomycetes* were significantly more abundant ($p < 0.05$) in Pg (Ni-HA) (59.6%, 5.8%, and 3.2%) than in Ps (nA) (7.9%, 0.7%, and 0.9%). Conversely, unclassified fungi and *Eurotiomycetes* were significantly more abundant ($p < 0.001$) in Ps (nA) (83.7% and 1.0%) than in Pg (Ni-HA) (24.2% and 0.3%). Specific classes like *Wallemiomycetes* (0.1%) and *Cystobasidiomycetes* (0.1%) were unique to Pg (Ni-HA) pulps, while *Ustilaginomycetes* (0.1%) and *Lecanoromycetes* (0.1%) were unique to Ps (nA) pulps.

In leaves, the proportions of unclassified fungi, *Eurotiomycetes*, *Pezizomycetes*, and *Agaricomycetes* were significantly higher ($p < 0.01$) in Ps (nA) (25.3%, 11.7%, 7.2%,

and 8.3%) than in Pg (Ni-HA) (19.6%, 0.4%, 0.5%, and 0.4%). *Dothideomycetes*, however, were significantly more abundant ($p < 0.0001$) in Pg (Ni-HA) (39.7%) compared to Ps (nA) (10.4%). Additionally, *Ramicandelaberomycetes* (0.7%), *Mortierellomycetes* (0.1%), *Rhizophydiomycetes* (0.1%), and GS14 (*Chytridiomycota* phylum 0.1%) were exclusive to Ps (nA), while *Lecanoromycetes* (0.1%) was unique to Pg (Ni-HA).

In the belowground compartments, unclassified fungi and *Sordariomycetes* were significantly more abundant ($p < 0.0001$) in Ps (nA) roots (49.1% and 19.1%) compared to Pg (Ni-HA) roots (13.2% and 5.3%). On the other hand, *Agaricomycetes* were significantly more prevalent ($p < 0.0001$) in Pg (Ni-HA) roots (70.6%) than in Ps (nA) roots (12.4%). Specific classes like *Atractiellomycetes* (0.1%) and GS35 (*Ascomycota* phylum 0.2%) were found only in Ps (nA) roots.

Finally, *Pezizomycetes* (1.2%), *Ramicandelaberomycetes* (0.3%), and *Geoglossomycetes* (0.1%) were exclusive to Pg (Ni-HA) rhizospheric soil, while *Spizellomycetes* (0.1%) and *Saccharomycetes* (0.1%) were unique to Ps (nA) rhizospheric soil.

ASV distributions

Overall, 5602 ASVs were classified as Bacteria, while 4584 were classified as Fungi (Fig. 7).

The Venn diagram showed that half of the bacterial ASVs (657 + 2188 = 50.88%) were shared between Pg (Ni-HA) and Ps (nA), while 1092 ASVs (19.5%) were strictly associated with bulk soil. Additionally, 17.1% (551 + 409) were specific to Ps (nA), and 12.6% (486 + 219) were specific to Pg (Ni-HA). For fungal ASVs, 32.9% (1132 + 377) were specific to Ps (nA), and 19.0% (644 + 228) were specific to Pg (Ni-HA).

When analysing the distribution of specific ASVs in Pg (Ni-HA) or Ps (nA), a similar trend was observed across all subsets of the libraries: the majority of ASVs were specifically associated with belowground compartments (roots and rhizospheric soil) (Fig. 7). Specifically, 97.5% (44.7% + 21.7% + 31.1%) of bacterial ASVs and 80.8% (54.1% + 19.5% + 7.2%) of fungal ASVs were uniquely associated with Pg (Ni-HA), while 97.4% (65.4% + 19.9% + 12.1%) of bacterial ASVs and 64.2% (44.9% + 12.6% + 6.7%) of fungal ASVs were associated with Ps (nA). For aboveground compartments (leaves, pulps, seeds), the proportion of specific ASVs varied between 0% and 8.1%, except for specific fungal ASVs in Ps (nA) leaves (26.4%).

Specific taxonomic biomarkers of *Psychotria gabriellae* (Pg, Ni-HA) and *Psychotria semperflorens* (Ps, nA) at genus level

The intraspecific analysis of specific microbiotas at the genus level identified a total of 49 bacterial biomarkers for Pg (Ni-HA) and 74 for Ps (nA). For fungal biomarkers, 78 were identified for Pg (Ni-HA), while 126 were found for Ps (nA) (Table 3).

Seeds of Pg (Ni-HA) were the only compartment that did not exhibit any fungal biomarkers. Overall, Ps (nA) had nearly twice as many biomarkers across all libraries combined compared to Pg (Ni-HA).

A noteworthy observation was the high proportion of unclassified genera among bacterial biomarkers, accounting for 53.1% in Pg (Ni-HA) and 62.2% in Ps (nA), representing the majority of the total bacterial biomarkers. In contrast, unclassified genera were less prevalent among fungal biomarkers, making up 32.1% in Pg (Ni-HA) and 26.2% in Ps (nA).

Co-Occurrence Networks Between Specific Microbiotas of *Psychotria gabriellae* (Pg, Ni-HA) and *Psychotria semperflorens* (Ps, nA)

Except for Pg (Ni-HA) seeds and Ps (nA) leaves, all compartments met the Spearman correlation criteria ($R > 0.6$ with p-value < 0.05) required (Fig. 8).

Each network exhibited low connectance (0.03–0.14), indicating that less than 1.4% of possible significant positive correlations were present (Table 4).

However, belowground compartment networks demonstrated a high average degree (17.60–41.95), suggesting that individual ASVs had significant positive correlations within these networks. This was indicative of complex and interconnected networks with numerous modules, as observed in the belowground compartments. Indeed, these networks exhibited high modularity (ranging from 0.70 to 0.92), reflecting substantial community structuring. Specifically, the number of modules was greater in belowground compartments compared to aboveground ones: Ps (nA) roots (54 modules), Pg (Ni-HA) roots (20 modules), Pg (Ni-HA) rhizospheric soil (19 modules), Ps (nA) rhizospheric soil (18 modules), Ps (nA) pulps (13 modules), Pg (Ni-HA) leaves (10 modules), Pg (Ni-HA) pulps (9 modules), and Ps (nA) seeds (5 modules). Concerning the centralisation degrees, they ranged between 0.04 and 0.09, suggesting that no single ASV played a dominant role in any network. Additionally, betweenness centrality metrics did not exceed 0.18, indicating that no ASV was crucial for global interactions within networks.

Except for the Pg (Ni-HA) leaves network, each network exhibited some modules containing bacterial and fungal biomarkers, which we highlighted in the previous section (Table 5).

In total, 62 biomarkers were present across all the networks, with only 11 not showing a specific association with any particular network (*Diaporthe*, *Acidothermus*, *Bryobacter*, *Gemmata*, SWB02 (*Proteobacteria* phylum), *Candidatus Solibacter*, *Mycena*, *Candidatus Udaeobacter*, *Pirellula*, *Entoloma*, and *Hygrocybe*). Aside from the

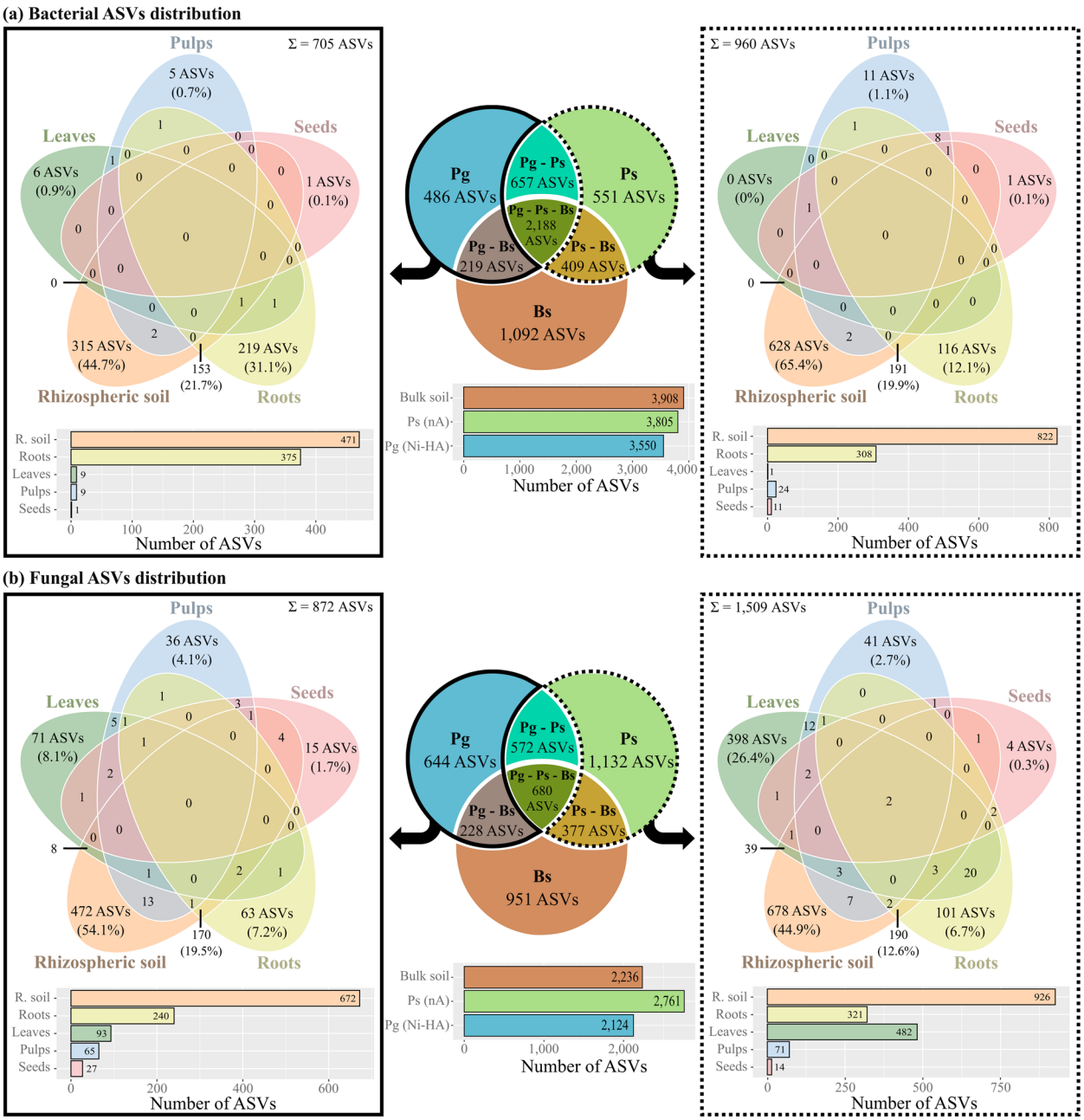

Fig. 7 Venn diagrams of (a) bacterial ASV distribution and (b) fungal ASV distribution. (Pg = *Psychotria gabriellae* (Ni-HA), Ps = *Psychotria semperflorens* (nA), Bs = bulk soil, and r. soil = rhizospheric soil)

Pg (Ni-HA) leaves network, which contained only fungal biomarkers–specifically a co-occurrence of *Colletotrichum* and *Diaporthe*–the other networks presented both fungal and bacterial biomarkers. In some cases, these were associated with each other within one or more modules. For instance, in a non-exhaustive sense, *Acidothermus*, *Bryobacter*, and *Gemmata* in the Pg (Ni-HA) roots network; *Bryobacter*, *Castanediella*, and *Candidatus Solibacter* in the Ps (nA) roots network; *Candidatus sp.*, *Entoloma*, and *Fusarium* in the Pg (Ni-HA) rhizospheric soil network; and *Pedomicrobium*, *Entoloma*, and *Hygrocybe* in the Ps (nA) rhizospheric soil network. In contrast, all biomarkers present in the Ps (nA) pulps network (*Methylobacterium-Methylorubrum*, *Derxomyces*, *Neocucurbitaria*, and *Diaporthe*) were not associated within the same modules. Lastly, no biomarkers were present in the Ps (nA) seeds or Pg (Ni-HA) pulps networks.

Table 3 Overview of LEfSe analysis results

Species[a]	Kingdom	Compartment	Number of biomarkers[b]	Number of "unclassified" biomarkers	LDA score range
Pg (Ni-HA)	*Bacteria*	Seeds	1 (2.0%)	0	5.3
		Pulps	2 (4.1%)	0	5.5–5.7
		Leaves	11 (22.4%)	5 (45.5%)	4.2–5.0
		Roots	18 (36.7%)	9 (50.0%)	4.1–4.9
		Rhizospheric soil	17 (34.7%)	12 (70.6%)	4.0–4.9
		Summary	49 (100.0%)	26 (53.1%)	4.0–5.7
	Fungi	Seeds	0	0	
		Pulps	7 (9.0%)	3 (42.9%)	4.0–5.3
		Leaves	34 (43.6%)	6 (17.6%)	3.1–5.6
		Roots	19 (24.4%)	9 (47.4%)	3.2–5.2
		Rhizospheric soil	18 (23.1%)	7 (38.9%)	3.4–5.2
		Summary	78 (100.0%)	25 (32.1%)	3.1–5.6
Ps (nA)	*Bacteria*	Seeds	2 (2.7%)	1 (50.0%)	4.8–5.6
		Pulps	6 (8.1%)	2 (33.3%)	4.2–5.1
		Leaves	11 (14.9%)	4 (36.4%)	3.6–4.5
		Roots	14 (18.9%)	8 (57.1%)	3.8–4.8
		Rhizospheric soil	41 (55.4%)	31 (75.6%)	3.7–4.7
		Summary	74 (100.0%)	46 (62.2%)	3.6–5.6
	Fungi	Seeds	3 (2.4%)	1 (33.3%)	4.60–5.63
		Pulps	12 (9.5%)	2 (16.7%)	3.95–4.90
		Leaves	61 (48.4%)	10 (16.4%)	2.88–4.57
		Roots	34 (27.0%)	14 (41.2%)	3.02–5.25
		Rhizospheric soil	16 (12.7%)	6 (37.5%)	3.30–4.87
		Summary	126 (100.0%)	33 (26.2%)	2.88–5.63

LEfSe parameters: alpha threshold = 0.05; taxa level = genus; *p*-value adjustment method = Bonferroni

[a] Pg = *Psychotria gabriellae* (Ni-HA) and Ps = *Psychotria semperflorens* (nA)

[b] Refers to significant genus

Table 4 Graph network properties

Graph network[a]	Edges	Vertices	Connectance	Average degree	Modularity	No. modules	Centralisation degree	Betweenness centrality
Ps (nA) seeds	14	14	0.15	2.00	0.71	5	0.08	0.00
Pg (Ni-HA) pulps	149	51	0.12	5.84	0.82	9	0.04	0.00
Ps (nA) pulps	163	57	0.10	5.72	0.71	13	0.09	0.00
Pg (Ni-HA) leaves	117	49	0.10	4.78	0.83	10	0.05	0.00
Pg (Ni-HA) roots	7,000	549	0.05	25.50	0.80	20	0.09	0.18
Ps (nA) roots	4,048	460	0.04	17.60	0.92	54	0.04	0.00
Pg (Ni-HA) r. soil	17,500	1,077	0.03	32.50	0.70	19	0.06	0.02
Ps (nA) r. soil	34,755	1,657	0.03	41.95	0.71	18	0.05	0.02

[a] Pg = *Psychotria gabriellae* (Ni-HA), Ps = *Psychotria semperflorens* (nA), and r. soil = rhizospheric soil

Discussion

How are metallophyte microbiotas structured?

Our work provides valuable evidence regarding the structure of the microbiotas of *Psychotria gabriellae* (Pg, Ni-HA) and *Psychotria semperflorens* (Ps, nA). By analysing alpha and beta diversities, the distributions of microbial ASVs, and relative abundance profiles, we revealed that the host plant and/or its compartment influence microbial communities depending on the microbial kingdom.

To the best of our knowledge, we are the first to dissect *in situ*, through a systematic compartment-specific

Table 5 Summary of microbial biomarkers, identified using the LEfSe method at the genus level, present in the co-occurrence networks of *Psychotria gabriellae* (Pg, Ni-HA) and *Psychotria semperflorens* (Ps, nA)

Graph network	Biomarkers at genus level	Kingdom	Module number
Ps (nA) pulps	***Methylobacterium-Methylorubrum***	*Bacteria*	11
	Derxomyces	*Fungi*	3
	Diaporthe	*Fungi*	2, 4, and 9
	Neocucurbitaria	*Fungi*	13
Pg (Ni-HA) leaves	***Ceratosphaeria***	*Fungi*	10
	Colletotrichum	*Fungi*	2 and 8
	Diaporthe	*Fungi*	8 and 9
Pg (Ni-HA) roots	*Acidothermus*	*Bacteria*	3 and 4
	Actinophytocola	*Bacteria*	2 and 20
	Bryobacter	*Bacteria*	2, 3, 6, 8, 11, and 12
	Gemmata	*Bacteria*	3, 4, 5, 7, 11, and 14
	Niastella	*Bacteria*	2, 3, 11, 12, and 13
	SWB02	*Bacteria*	5 and 8
	Diluviicola	*Fungi*	6
	Endoradiciella	*Fungi*	9
	Gymnopus	*Fungi*	6
	Junghuhnia	*Fungi*	19
	Leohumicola	*Fungi*	9 and 11
	Neonectria	*Fungi*	9
Ps (nA) roots	*Acidothermus*	*Bacteria*	18, 22, and 24
	Bryobacter	*Bacteria*	1, 3, 9, 11, 12, 14, 23, and 27
	Candidatus Solibacter	*Bacteria*	2, 3, 6, 12, and 17
	Mycobacterium	*Bacteria*	25 and 26
	Bourdotigloea	*Fungi*	8 and 23
	Castanediella	*Fungi*	1 and 2
	Cladophialophora	*Fungi*	7 and 13
	Mycena	*Fungi*	1
	Thozetella	*Fungi*	32
	Verruconis	*Fungi*	28
Pg (Ni-HA) rhizospheric soil	*Candidatus Solibacter*	*Bacteria*	6, 7, 8, 9, 10, 11, 12 and 13
	Candidatus Udaeobacter	*Bacteria*	3, 5, 6, 9, 10, 12, and 13
	Nocardioides	*Bacteria*	2 and 6
	Pirellula	*Bacteria*	10 and 12
	Calceomyces	*Fungi*	19
	Clonostachys	*Fungi*	2, 3, 15
	Entoloma	*Fungi*	2, 5, 6, 9, 12, and 13
	Fusarium	*Fungi*	3, 7, and 13
	Hygrocybe	*Fungi*	2, 6, and 12
	Mycena	*Fungi*	2, 5, and 13
	Pidoplitchkoviella	*Fungi*	2 and 10
	Pluteus	*Fungi*	2, 12, and 13
	Pulvinula	*Fungi*	2
	Talaromyces	*Fungi*	2
	Virgaria	*Fungi*	1, 2, 5, 7, and 13

Table 5 (continued)

Graph network	Biomarkers at genus level	Kingdom	Module number
Ps (nA) rhizospheric soil	*Candidatus Udaeobacter*	*Bacteria*	1, 2, 3, 4, 5, 7, 10, 11, and 13
	Gemmata	*Bacteria*	2, 8, 11, 13, 16, and 18
	Pedomicrobium	*Bacteria*	2, 3, 4, 8, and 9
	Pirellula	*Bacteria*	2, 4, 9, 11, 12, and 13
	Reyranella	*Bacteria*	2, 3, and 16
	Rhodoplanes	*Bacteria*	1, 2, 7, and 11
	SM1 A02	*Bacteria*	1, 2, 3, 7, and 12
	SWB02	*Bacteria*	2 and 7
	Aphanoascus	*Fungi*	3 and 4
	Clitopilus	*Fungi*	2, 7, 9, 13
	Entoloma	*Fungi*	2, 3, 7, 9, 12, and 13
	Geastrum	*Fungi*	3 and 6
	Humicola	*Fungi*	2, 3, and 7
	Hygrocybe	*Fungi*	2, 3, 7, 9, 10, 13
	Mariannaea	*Fungi*	2
	Pilidium	*Fungi*	2 and 3
	Trichoderma	*Fungi*	2, 3, and 11
	Volutella	*Fungi*	1, 2, and 7

Genera in bold are those present in only one network

comparative approach, the structures and compositions of the fungal and bacterial microbiotas in relation to Ni hyperaccumulation or exclusion phenotypes of New Caledonian metallophytes. Moreover, we are the first to explore fungal and bacterial diversity within the pulps compartment of metallophytes. Therefore, this study provides the first comprehensive data on the microbiota across the entire fruit of Pg (Ni-HA) and Ps (nA).

Diversity of microbial communities in Psychotria gabriellae (Pg, Ni-HA) and Psychotria semperflorens (Ps, nA)

Alpha diversity indices effectively differentiate bacterial communities between above- and belowground compartments, with diversity decreasing from soil to endosphere [58]. Our study shows similar values for belowground compartments but lower diversity in aboveground compartments compared to the literature (see Additional file 6). Several factors may explain this reduction. Firstly, the use of primers not suited to our study may lead to either a mismatch between bacterial 16S rRNA genes and universal primers [59] and/or increased amplification of plant-derived sequences [60], which limits amplification and reduces detected diversity. In this study, we filtered 1,226,768 sequences affiliated with mitochondria or chloroplasts. The majority of these filtered sequences were represented by 2 ASVs (ASV5086_16S and ASV4803_16S), which accounted for an average of 90–92% of the reads in the plant compartments. This could led to an underestimation of bacterial diversity. Secondly, the lower diversity in aboveground compartments may reflect high niche specialisation, particularly in seed endophytes. The high Ni concentrations in Pg (Ni-HA) leaves (21,400 $\mu g.g^{-1}$) and seeds (9810 $\mu g.g^{-1}$) [61] may have driven the selection. Indeed, the bacterial genera present in these compartments appear to be well adapted to heavy metal (HM) stress and promote plant growth. *Methylobacterium*, abundant in Pg (Ni-HA) pulps (17.9%) and Ps (nA) pulps (30.2%) and seeds (1.2%) (see Additional file 2), enhances plant fitness [62, 63]. It also produces N-acyl-homoserine lactones, signaling molecules involved in quorum sensing, which may facilitate biofilm formation and endophyte colonization [64]. Other genera, including *Rhizobium*, *Frankia*, *Brevundimonas*, *Sphingobium*, *Sphingomonas*, *Novosphingobium*, *Bradyrhizobium*, *Bosea*, and *Labrys*, exhibit similar plant growth-promoting (PGP) traits and HM tolerance [65–72]. Some genera also modulate

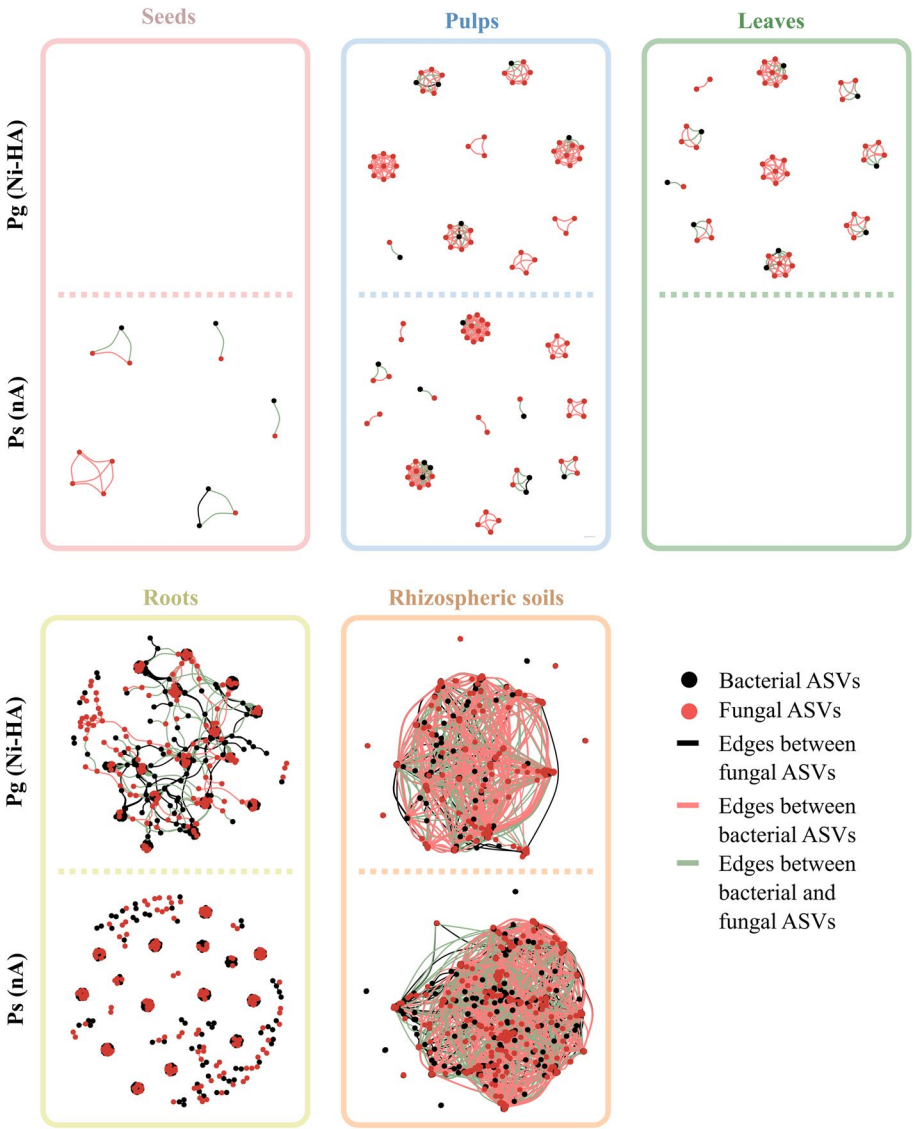

Fig. 8 Co-occurrence networks of significant positive correlations between specific microorganisms (bacteria and fungi) of *Psychotria gabriellae* (Pg, Ni-HA) and *Psychotria semperflorens* (Ps, nA) in leaves, pulps, seeds, roots, and rhizospheric soils

metal uptake [72, 73]. Their competitive advantages and pre-existing presence in micro niches may partly explain the observed low diversity. A third hypothesis concerns bacterial-fungal competition in leaf compartments. The high ASV count in fungal leaf endophytes (90 in Pg (Ni-HA) and 149 in Ps (nA)) suggests competition with bacteria. Notably, abundant genera in Pg (Ni-HA) and Ps (nA) include antimicrobial-producing fungi such as *Pseudocercospora* (30.6% in Pg (Ni-HA)), *Colletotrichum* (11.4% in Pg (Ni-HA), 4.8% in Ps (nA)), *Anthracobia* (5.9% in Ps (nA)), *Talaromyces* (5.0% in Ps (nA)), and *Penicillium* (4.8% in Ps (nA)) [74–79]. Lastly, a low diversity in seeds is in agreement with findings of Ancousture et al. [19], who have shown a relatively low richness of the HA seeds bacterial communities. Moreover, the same authors have also demonstrated that significant differences in bacterial community diversity across hyperaccumulator seed families may be observed, which could explain the lower diversity observed in the species studied. However, further tests are needed to confirm if the New Caledonian *Psychotria* species studied belong to families with inherently reduced microbial diversity.

Regarding fungal communities, our results align with literature findings to varying degrees, depending on the study and compartments examined (see Additional

file 6). Although we observed higher diversity in some compartments compared to the literature, we may have underestimated the overall diversity of fungal communities. One-third of ASVs (33.2%) were unclassified at the kingdom level, suggesting we might be overlooking fungal species that have not yet been sequenced and are therefore absent from international databases. This knowledge gap is especially relevant to New Caledonia and tropical regions in general [80, 81]. New Caledonia's ultramafic substrates are well known for their high levels of endemism and microendemism [82, 83]. While research typically emphasises the endemism and microendemism of vascular organisms, microorganisms associated with these soils can also exhibit a significant proportion of native taxa. For example, a study by Carriconde et al. [84] on ectomycorrhizal diversity in the New Caledonian tropical rainforest on ultramafic soils reported that up to 95% of taxa had only been recorded in New Caledonia. Therefore, our study emphasises the importance of implementing a comprehensive sequence database to better characterise New Caledonian metallophytes and their microbiomes.

Composition of microbial communities in Psychotria gabriellae (Pg, Ni-HA) and Psychotria semperflorens (Ps, nA)

The bacterial communities of both plant species are dominated by *Alphaproteobacteria*. At the class level, bacterial profiles differ between aboveground and belowground compartments, which reflects the observed patterns in alpha diversity. Belowground compartments primarily consist of *Alphaproteobacteria*, *Actinobacteria*, *Acidobacteria*, *Planctomycetes*, and *Acidimicrobia*. These profiles are consistent with those found in Ni-hyperaccumulator species on ultramafic soils [85]. Studies by Lopez et al. [85] and Gourmelon et al. [34] similarly identified *Proteobacteria*, *Acidobacteria*, *Chloroflexi*, and *Planctomycetes* in hyperaccumulator rhizospheres (Additional file 2). In contrast, Durand et al. [86] found that *Actinobacteria*, *Alphaproteobacteria*, *Gammaproteobacteria*, and *Betaproteobacteria* were dominant taxa in poplar roots on Hg-contaminated sites, while *Gammaproteobacteria* dominated *Odontarrhena chalcidica* roots under Ni pressure [87]. However, in the seeds and leaves compartments of New Caledonian *Psychotria* species, there are slight deviations from those reported bacterial profiles. For example, Ancousture et al. [19] revealed that seeds of various hyperaccumulator (HA) and non-HA species were predominantly associated with *Gammaproteobacteria*; a finding that was subsequently confirmed in *Odontarrhena* seeds by Durand et al. [17]. In contrast, the present study found that *Alphaproteobacteria* to be dominant in the seeds of both species, with smaller proportions of *Fusobacteriia* in Pg (Ni-HA) and *Gammaproteobacteria* in Ps (nA). In the leaves compartment, we observed a dominance of *Proteobacteria*, *Fusobacteriota*, and *Actinobacteriota* in Pg (Ni-HA), while Ps (nA) leaves exhibited a predominance of *Alphaproteobacteria*. Jiang et al. [88] reported that *Actinobacteria* and *Proteobacteria* were predominant in *Sedum alfredii* leaves, alongside minor *Firmicutes* and *Bacteroidetes*, while Durand et al. [89] found that poplar leaves from Hg-contaminated sites were mainly composed of *Alphaproteobacteria*, *Bacteroidetes*, *Actinobacteria*, and *Deinococcus*.

We also observed notable differences in fungal community profiles at the class level across compartments and species. Chen et al. [90] reported a dominance of *Ascomycota* and *Basidiomycota*, with smaller proportions of unclassified fungi and *Mortierellomycota* in the rhizosphere of *Ricinus communis* at an abandoned mining site. Although the same phyla were present in our study, we found that *Mortierellomycota* and *Basidiomycota* were predominant in Pg (Ni-HA) with smaller proportions of *Ascomycota* and unclassified fungi, while *Ascomycota* was dominant in Ps (nA), followed by *Basidiomycota* and *Mortierellomycota*. The higher proportion of *Mortierellomycota* in our rhizospheric samples was not noted by Gourmelon et al. [34] in their characterisation of fungal diversity in multiple rhizospheres on New Caledonian ultramafic substrates. Similarly, Zhang et al. [91] found lower proportions of *Mortierellomycota*, with a dominance of *Ascomycota*, in their study on soil fungal diversity under Ni pressure. Sharma et al. [92] reported a dominance of *Ascomycota* in the roots of *Arabis alpina*, while we observed a predominance of *Basidiomycota*, followed by *Ascomycota* and unclassified fungi, in Pg (Ni-HA) roots. In contrast, Ps (nA) roots were primarily composed of *Ascomycota*, *Basidiomycota*, and unclassified fungi. The dominance of *Ascomycota* in roots has also been reported in other studies [90, 93]. In leaves and seeds, we found that *Ascomycota* and *Basidiomycota* were predominant, consistent with other studies [88, 90, 92, 94].

Structure of microbial communities in Psychotria gabriellae (Pg, Ni-HA) and Psychotria semperflorens (Ps, nA)

Despite similar class composition in the belowground compartments of Pg (Ni-HA) and Ps (nA), we observed that bacterial communities in the rhizosphere primarily clustered according to the compartment type. The average number of observed ASVs does not significantly differentiate the communities between species in these compartments. Of the total 5602 ASVs, 2845 are shared between species (see Additional file 7). Of this core group, 98.7% are exclusively associated with the rhizosphere. Examining the distribution of species-specific

ASVs in Pg (Ni-HA) and Ps (nA) reveals that a majority are exclusively present in the roots (31.1% for Pg (Ni-HA) and 12.1% for Ps (nA)) and in rhizospheric soil (44.7% for Pg (Ni-HA) and 65.4% for Ps (nA)). Similar clustering by root and soil compartments has been observed in other studies [86, 95]. In contrast to belowground compartments, the beta diversity analysis of aboveground compartments did not group all compartments together. Only the fruits of Ps (nA) and the pulps of Pg (Ni-HA) were distinctly separated. This separation was not always evident in aboveground compartments; for instance, in grapevine, the grape, leaf, and flower compartments clustered together [96]. The leaves of Ps (nA) and the seeds of Pg (Ni-HA) were scattered among themselves (clusters k6_B and k7_B) and with the leaves of Pg (Ni-HA) (cluster k8_B) (see Additional file 5). The dispersion of these samples in the beta analysis can be attributed to their heterogeneity, particularly within the leaves compartment, where not all ASVs were consistently present in each replicate. This reduced distinction between aboveground compartments aligns with findings by Durand et al. [86] in poplar, where stem and leaf compartments showed less marked dissimilarity ($R = 0.61$; $p = 0.001$) compared to roots and soil ($R = 1$; $p = 0.001$) on Hg-contaminated sites. Additionally, the dispersion is influenced by the fact that most ASVs associated with these samples are shared across compartments. Analysis of ASV distribution in Ps (nA) revealed that, out of 24 ASVs associated with pulps, 11 are exclusive to pulps, while 8 are strictly shared between pulps and seeds (out of a total of 11 ASVs associated with seeds). This distribution likely accounts for the distinct clustering of Ps (nA) fruits samples. Similarly, in Pg (Ni-HA), we observed that 5 of the 9 ASVs found in pulps are unique to this compartment (with an average of 8 ± 2 ASVs in Pg (Ni-HA) pulps), potentially accounting for the distinct clustering of Pg (Ni-HA) pulps samples.

In contrast to bacterial communities, fungal communities are distinctly grouped by species and compartment, including rhizospheric soil, roots, leaves, and fruits (seeds and pulps). This grouping is primarily explained by the distribution of ASVs, where compartment- and species-specificity are most pronounced.

Is there a distinct microbial signature associated with plant exclusion and hyperaccumulation phenotypes?

A total of 1577 and 2469 microbial ASVs were strictly associated with *Psychotria gabriellae* (Pg, Ni-HA) and *Psychotria semperflorens* (Ps, nA), respectively. Using an integrated approach that combines linear discriminant analysis and graph networks, we identified specific biomarkers for Pg (Ni-HA) and Ps (nA) (Table 5, Fig. 9).

As highlighted below, several specific and common biomarkers identified are known to secrete molecules—such as siderophores, organic acids, hydrogen cyanide (HCN), and exopolysaccharides (EPS)—that complex metals, sorb Ni, enhance plant metal stress tolerance, or even amplify metal accumulation (Tables 6 and 7).

Common biomarkers that may explain the adaptation of both Psychotria species to ultramafic constraints

The genera *Diaporthe* and *Mycena*, which are common biomarkers for both Pg (Ni-HA) and Ps (nA) (Table 6), are both known to exhibit tolerance to Ni [97, 98]. The genus *Diaporthe*, a biomarker in the leaves of Pg (Ni-HA) and the pulps of Ps (nA), plays a crucial role in Ni accumulation in the Ni-hyperaccumulating species *Noccaea caerulescens* and *N. goesingensis* [97]. Inoculation of plantlets with the *Phomopsis* strain (the anamorph form of *Diaporthe*) increases Ni accumulation in the roots and leaves of these two species under controlled conditions. In the case of *N. caerulescens*, inoculation with the *Phomopsis* strain also induced the overexpression of genes associated with metal transporters. This study, conducted by Wazny et al. [97], underscores the complexity of the hyperaccumulation process in plants. This specific HA mechanism seems to depend not only on the plant but also on its microbiome. Indeed, depending on the source of the inoculated *Phomopsis* strain, Ni accumulation in *N. caerulescens* varies. A significant increase in Ni accumulation is observed only when the inoculated strain is native to the plant (i.e., isolated from the plant using culture-dependent methods). The presence of this genus in the foliar compartment of Pg (Ni-HA) could, therefore, potentially promote the Ni hyperaccumulation phenotype in Pg (Ni-HA). Furthermore, this genus also exhibits numerous growth-promoting effects, which could support the establishment and/or development of Pg (Ni-HA) and Ps (nA) on ultramafic substrates [89].

Specific biomarkers of Psychotria gabriellae (Pg, Ni-HA) that may explain its Ni-hyperaccumulation phenotype

Several biomarkers associated with the rhizosphere of Pg (Ni-HA) exhibit sorption capacities for different HM, such as *Fusarium* [117] and *Talaromyces* [108] (Table 7). These sorption capacities can render HM, other than Ni, present in the soil unavailable and thus reduce metal-induced stress and the accumulation of HM in the plant. Additional microbial-assisted mechanisms could also assist in reducing metal-induced stress in the plant. For example, the *Colletotrichum* genus, which is a biomarker in Pg (Ni-HA) leaves in our study, is known for producing

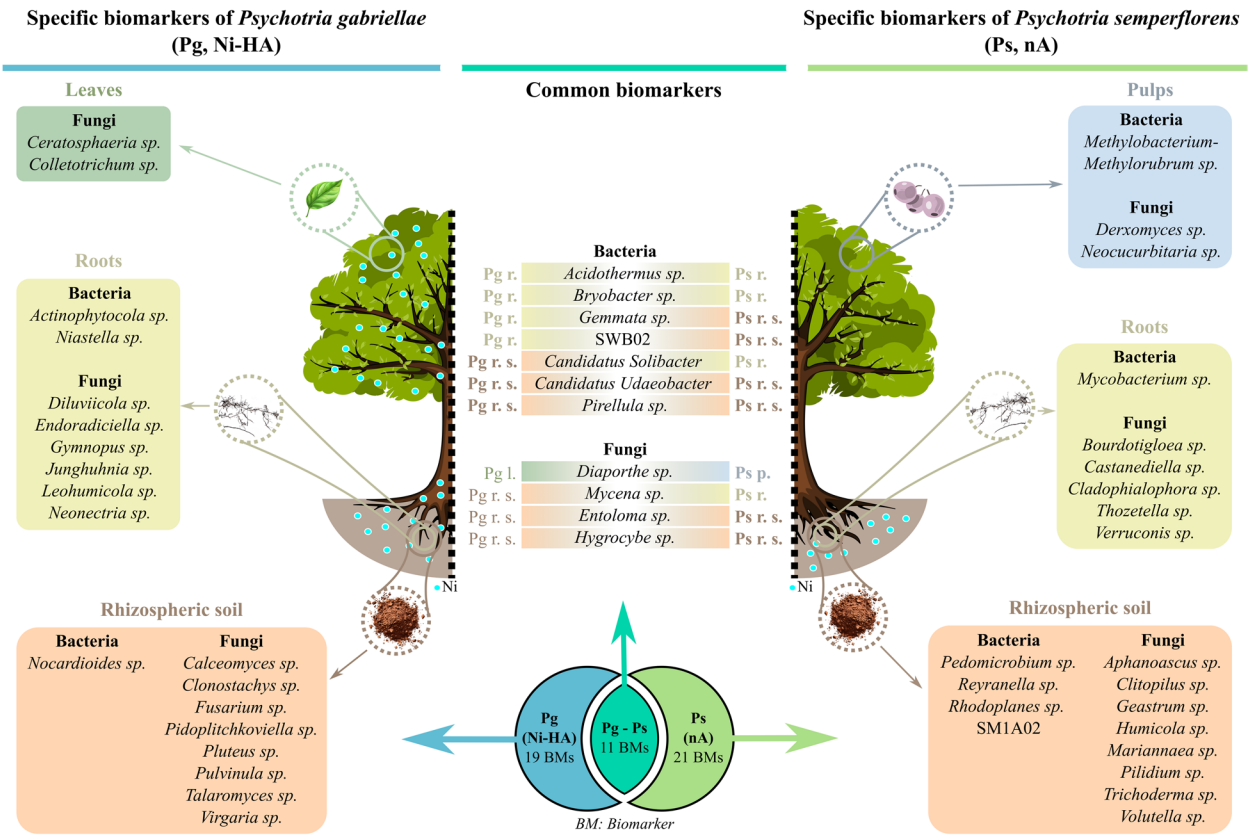

Fig. 9 Summary diagram of the results obtained from the analysis performed (LEfSe + graph network) on the specific microbiotas of *Psychotria gabriellae* (Pg, Ni-HA) and *Psychotria semperflorens* (Ps, nA). r.: roots; r. s.: rhizospheric soil; l.: leaves; p.: pulps; Ni: nickel

Table 6 Overview of the effects on plant growth and adaptation to nickel stress, as well as nickel tolerance, of genera identified as biomarkers in *Psychotria gabriellae* (Pg, Ni-HA) and *Psychotria semperflorens* (Ps, nA) (non-exhaustive listing)

Species and compartment	Biomarker[a]	Environment	PGP effect	Ni-tolerance and effect on plant under metal stress[b]
Pg (Ni-HA) leaves / Ps (nA) pulps	*Diaporthe* (F)	Endophytes from *Noccaea caerulescens* (Ni-HA population and Pb–Zn adapted population from Spain), *Noccaea goesingensis* (Ni-HA population from Austria and non-toxic metal-adapted population from Spain), and *Odontarrhena serpyllifolia* (Ni-HA from Spain) [97] Isolated from roots of *Festuca rubra* subsp. *pruinosa* (Spain) [89]	Siderophore production [89]	Ni-tolerance (3000 µM) [97] ↑ [Ni] in shoots and roots of *Noccaea caerulescens* (Ni-HA) (with an inoculation of native strain) [97] ↑ [Ni] in shoots and roots of *Noccaea goesingensis* (Ni-HA) (with an inoculation of native or foreign strain) [97] ↑ gene expression of *IRT1*, *ITR2*, and *ZIP5* in *Noccaea caerulescens* (Ni-HA) under Ni pressure. [97]
Pg (Ni-HA) rhizospheric soil / Ps (nA) roots	*Mycena* (F)			Ni-tolerance [98]

[a] (F) = fungal genus

[b] *IRT1* = IRON REGULATED TRANSPORTER 1 gene; *IRT2* = IRON-REGULATED TRASNPORTER 2 gene; *ZIP5* = ZINC TRANSPORTER 5 PRECURSOR gene; *Ni-HA* = Ni-hyperaccumulator

1-aminocyclopropane-1-carboxylate (ACC) deaminase (ACCD) [100]. This enzyme degrades ACC [118], a precursor of ethylene, which is a hormone produced in response to metal stress [119]. When present in high concentrations, ethylene can inhibit growth and induce senescence processes [120]. ACCD production by

Table 7 Overview of the effects on plant growth and adaptation to nickel stress, as well as nickel tolerance, of genera identified as biomarkers in *Psychotria gabriellae* (Pg, Ni-HA) or *Psychotria semperflorens* (Ps, nA) (non-exhaustive listing)

Species and compartment	Biomarker[a]	Environment[b]	PGP effect[c]	Ni-tolerance and effect on plant under metal stress[d]
Ps (nA) pulps	*Neocucurbitaria* (F)	Endophyte of *Noccaea caerulescens* (Ni-HA, from Pb–Zn adapted population) (Spain) [97]		↑ [Ni] accumulation in roots and leaves of *Noccaea caerulescens* (Ni-HA) [97]
	Methylobacterium-Methylorubrum (B)	Isolated from the phyllosphere of *Oryza sativa* [62] Isolated from stem and leaf of *Oryza sativa* (Korean) [63] Isolated from the rhizosphere of *Thlaspi goesingense* (Ni-HA) in serpentine soil (Austria) [99]	Siderophore production [99] ACCD activity [62, 63, 99]	Genes involved in HM biosorption or reduction of metal toxicity [62] Ni and Cd-tolerance and sorption abilities [63] ↓ [Ni] and [Cd] in roots and shoots of *Lycopersicon esculentum* under Ni/Cd stress [63] Ni-tolerance [99]
Pg (Ni-HA) leaves	*Colletotrichum (F)*	Leaf-endophytes of *Eupatorium triplinerve* (India) [100] Endophyte of *Plumbago zeylanica* (India) [101]	ACCD activity [100] Siderophore production [100, 101] EPS production [101] Organic acid production [101] HCN production [101]	
Ps (nA) roots	*Mycobacterium* (B)	Isolated from the rhizoplane of *Graminaceae* in grasses in HM-polluted water meadow soil (Italy) [102]	ACCD activity [102]	Cd, Zn, Co, and Ni-tolerance [102]
Pg (Ni-HA) rhizospheric soil	*Clonostachys* (F)	Saprotrophic fungi isolated from soil in a derelict Fe-Cu sulphide mine (Italy) [103]		Ni-tolerance [103]
	Fusarium (F)	Isolated from textile-dye contaminated soil (India) [104] Isolated from agricultural soil (Egypt) [105] Isolated from landfill soil (Malaysia) [106]		Cr, Ni, Pb and Cd-accumulation [104] Can be used to remove Cu^{2+}, Pb^{2+}, Co^{2+}, Cd^{2+}, Ni^{2+}, and Fe^{2+} from wastewater [105] In consortia ↑ [Cr], [Cu], [Mn], [Ni], [Pb], and [Zn] in shoots of *Alocasia calidora* [106]
	Talaromyces (F)	Isolated from waste sites (India) [107] Isolated from wastewater (Egypt) [108] Leaf-endophyte of *Rosmarinus officinalis* (Egypt) [109]		In consortia, can be used to remove Pb(II) and Ni(II) from industrial effluents [107] Can be used in consortia and *Paraserianthes falcataria* mycorrhizae for the phytoremediation of Ni and Pb [110] Ni-sorption abilities [108] ↓ [Cd], [Ni], [Cu], and [Zn] in *Triticum aestivum* under phytoremediation process [109]
	Nocardioides (B)	Isolated from unplanted serpentine soils (USA) [111]		HM-tolerance, including Ni, Cr, Cd, Pb, Cu, and Co [111] Has histidine-rich regions homologous to predicted metallohistidines in HM efflux transporters [112]
Ps (nA) rhizospheric soil	*Rhodoplanes* (B)	Identified in Au mining abandoned site (China) [113]		Presents genes encoding binding proteins, notably involved in Ni regulation (*ureG* and *ureC*) [113]
	Trichoderma (F)	Isolated from rhizosphere of *Pinus koraiensis* in contaminated mining soil (South Korea) [114] Isolated from rhizosphere of plants in polluted soil [115] Isolated from decaying feather [116]	ACCD activity [114, 115] Siderophore production [114, 115] HCN production [115]	As, Cu, Cd, Ni, Pb, and Zn-tolerance [114] ↑ growth of *Zea mays* under metal stress [114] Cd, Cr, Pb, and Ni-tolerance [115] ↑ Ni and Cd phytoextraction by *Brassica juncea* in Cd-Ni contaminated soils [116]

[a] (B) and (F) indicate a bacterial genus and a fungal genus, respectively

[b] HM = heavy metal; Ni-HA = Ni-hyperaccumulator

[c] ACCD = 1-aminocyclopropane-1-carboxylate deaminase, EPS = Exopolysaccharide, HCN = hydrogen cyanide

[d] *ureG* = urease accessory protein G gene, *ureC* = urease alpha subunit gene

microorganisms can therefore mitigate the impact of metal stress on the growth of the host plant. Interestingly, some *Colletotrichum* strains are also capable of producing HCN, EPS, and siderophores [10, 100, 101]; three compounds that can form complexes with metals, affecting their bioavailability [121–123]. All these mechanisms work together to promote the development of the host plant, even in the presence of metal stress.

Concerning the Ni hyperaccumulation trait in Pg (Ni-HA), several biomarkers associated with its rhizosphere are capable of inducing, in some species, an increase or decrease in the concentration of one or more HM in the foliar and/or root tissues of their host plants. For example, *Leohumicola*, which is a biomarker in Pg (Ni-HA) roots, can decrease Zn and Cd concentrations in the leaves of *Salix caprea* under metal stress [124]. *Fusarium*, which is a biomarker in the rhizospheric soil of Pg (Ni-HA), can increase Fe, Pb, and Zn concentrations in the roots of *Alocasia calidora*, as well as Cr, Cu, Mn, Ni, Pb, and Zn concentrations in the leaves [106]. Meanwhile, *Talaromyces*, also a biomarker in the rhizospheric soil of Pg (Ni-HA) in our study, can increase Cd concentration in *Arabidopsis thaliana* under Cd stress [125] and decrease concentrations of Cd, Ni, Cu, and Zn in *Triticum aestivum* during a phytoremediation process [109]. It is undeniable that these microbial genera exhibit metal tolerance/resistance mechanisms and play a role in metal bioavailability for the plant. Therefore, the microbial ecotypes specifically associated with Pg (Ni-HA) could influence its Ni hyperaccumulation phenotype. However, further studies are needed to confirm or refute these hypotheses. For instance, inoculation tests of Pg (Ni-HA) under metal stress conditions with cultivable strains isolated from this species could confirm the role played by certain microbial strains in the Ni-hyperaccumulation phenotype evolved by Pg (Ni-HA).

Specific biomarkers of Psychotria semperflorens (Ps, nA) that may explain its Ni-exclusion phenotype

As observed in Pg (Ni-HA), the rhizosphere of Ps (nA) also contains biomarkers with HM sorption capacities such as *Trichoderma* [114, 126] (Table 7). The *Mycobacterium* genus, a biomarker in Ps (nA) roots, exhibits numerous metal tolerances [102] and promotes root elongation in *Brassica napus* under Cd stress [127]. This growth-promoting effect in *B. napus* can be explained by its ability to produce ACCD [102]. This genus may thus mitigate metal stress in Ps (nA) on ultramafic soils.

The biomarkers present in the rhizospheric soil also exhibit interesting capacities that support the development of Ps (nA) despite metal stress. For instance, the *Clitopilus* genus increases potassium and nitrogen acquisition in certain plants [128, 129]. The *Mariannaea* genus is capable of synthesising selenium nanoparticles [130], which can contribute to plant growth and stress tolerance [131]. The genus *Trichoderma*, known for its tolerance and sorption capacities towards several heavy metals, displays a wide range of plant growth-promoting effects, notably the siderophore production [114, 132]. Depending on the species, this genus can either enhance or reduce metal accumulation in the host plant. For example, under Cd stress, it reduces Cd accumulation in *Cicer arietinum* [132]. In contrast, under Ni and Cd stress, inoculating *Brassica juncea* with *Trichoderma* increases the phytoextraction of Ni and Cd by the host plant [116]. This trend of enhancing metal accumulation in the host plant is also observed in *Zea mays*, where accumulation of As, Cd, Cu, Pb, and Zn in roots and shoots is increased [114]. These studies highlight the specificity of plant-microorganism associations, which, depending on the species and type of metal considered, can promote either metal accumulation or exclusion mechanisms in plants. Lastly, the genus *Rhodoplanes*, a biomarker of Ps (nA) roots, presents genes encoding binding proteins, notably involved in Ni regulation [133].

Additionally, the competitive advantages of the *Methylobacterium-Methylorubrum* genus could explain Ps (nA) ability to grow and thrive on ultramafic soils. As mentioned above, this genus exhibits numerous plant growth-promoting effects. Its presence as a biomarker in Ps (nA) pulps could potentially support the plantlet's establishment and development on ultramafic substrates [134]. In fact, Kwak et al. [62] identified genes involved in HM tolerance and even in reducing metal toxicity. In addition to its tolerance to HMs [99, 135, 136], this genus also displays sorption capacities for Ni and Cd [63]. Moreover, under metal stress, this genus can reduce Ni and Cd accumulation in the roots and shoots of *Lycopersicon esculentum* [63]. Therefore, *Methylobacterium-Methylorubrum* could play a key role in the establishment of Ps (nA) and in its Ni exclusion mechanism.

As with the Ni hyperaccumulation phenotype in Pg (Ni-HA), further studies are necessary to more precisely explore the role of Ps (nA) biomarkers in its development and Ni exclusion phenotype.

Conclusions

This study builds upon previous research focusing on the plant-specific aspects of *Psychotria gabriellae* (Pg, Ni-HA) and *Psychotria semperflorens* (Ps, nA) by introducing a microbial perspective on their different adaptive behaviours towards nickel. We aimed to explore whether microbial communities are shaped by plant compartments or by plant species themselves, and whether each species has a distinct microbial signature, which may contribute to the hyperaccumulation

or exclusion phenotypes. Our findings reveal a notably low bacterial diversity in aboveground compartments, which merits further exploration. We observed that bacterial communities are compartmentalised within the belowground compartments, while both compartments and plant species influence fungal communities. Both Pg (Ni-HA) and Ps (nA) exhibit unique microbial signatures that could enhance their respective phenotype of hyperaccumulation and exclusion (non-accumulation). However, further research on the functional roles of these specific microbiotas is now needed to confirm these findings. This study is pioneering in characterising the microbiota of these two New Caledonian species, and it would be valuable to include other Ni-accumulating or excluding species at the same site to determine if there is a common microbial core contributing to Ni-adaptive phenotypes. Future works, including studies on other Ni-HA from New Caledonia and comparisons with species from different ultramafic sites, will provide deeper insights into the site-specific effects and broader microbial patterns.

Supplementary Information

The online version contains supplementary material available at https://doi.org/10.1186/s40168-025-02098-7.

Additional file 1: Detailed protocol of DNA extraction using an adapted CTAB method

Additional file 2: Averages of relative abundances at the phylum, class, and genus levels, along with stacked bar representations (for phyla and genera) and relative abundance statistics (for classes)

Additional file 3: Complete results of the LEfSe analysis conducted on the specific microbiotas of *P. gabriellae* (Pg, Ni-HA) and *P. semperflorens* (Ps, nA)

Additional file 4: Complete results of the graph network analysis, along with the ASV composition of each module within each graph network

Additional file 5: The merge fusion figures and hierarchical clustering

Additional file 6: Alpha diversity indices found in the literature for bacterial and fungal communities

Additional file 7: Venn diagrams of microbial core distribution

Acknowledgements
We are sincerely grateful to the South Province of New Caledonia and the owner of the Mont Koghi site (private property) for granting permission to sample *Psychotria* species. We express our gratitude to the MACROGEN team for conducting Illumina MiSeq sequencing. Our thanks also go to Adrien Thomas, Alizée Le Floc'h, Valérie Medevielle, Nina Brunet, and Mathilde Memeteau for their assistance during the sampling process. Finally, we extend our gratitude to Rodrigue Govan and Romane Scherrer for their expertise in Linux.

Authors' contribution
VBS conceptualised and designed the study. VBS and LG acquired funding for the project. JD, SG, LG, and VBS carried out the sampling. JD and SG prepared the samples for eDNA extraction. JD performed the eDNA extractions, bioinformatic treatments, statistical analysis, data visualisation, figure editing, and wrote the original manuscript draft. GL supervised the bioinformatics and statistical analyses. VBS, LG, GL, and SG reviewed the draft. All authors read and approved the final manuscript.

Funding
This work was supported by the Doctoral School of Pacific (EDP) of the University of New Caledonia (PhD research grant to Julie DIJOUX). Funding for this study was provided by a local project supported by the CRESICA (Consortium for the research, higher education and innovation in New Caledonia) as part of the "DEPOLEAU" project and by the Fonds Pacific fundings on the two projects: "Pacific Nickelators" (Project N°1795) and "MATRISS" (Project N°2330). We are also grateful to the PIURN (Pacific Island Universities Research Network) who supported this work via a dedicated funding through the project "Pacific Nickelators 2" as well as to the University of New Caledonia and the Institute of Exact and Applied Sciences for their strong support throughout the course of this project.

Data availability
The raw sequencing reads are available in the NCBI SRA database under BioProject PRJNA1157462. All scripts used in this study are available at https://github.com/juliedijoux/PgxPs_article.git.

Declarations

Ethics approval and consent to participate
Not applicable.

Consent for publication
Not applicable.

Competing interests
The authors declare no competing interests.

Author details
[1]Institute of Exact and Applied Sciences, University of New Caledonia, 145 Avenue James Cook, Noumea, New Caledonia, BP R4, 98851.

Received: 5 November 2024 Accepted: 24 March 2025
Published online: 04 May 2025

References

1. Hossain MA, Piyatida P, da Silva JAT, Fujita M. Molecular mechanism of heavy metal toxicity and tolerance in plants: central role of glutathione in detoxification of reactive oxygen species and methylglyoxal and in heavy metal chelation. J Bot. 2012;2012:1–37.
2. Ghori NH, Ghori T, Hayat MQ, Imadi SR, Gul A, Altay V, et al. Heavy metal stress and responses in plants. Int J Environ Scie Technol. 2019;16(3):1807–28. https://doi.org/10.1007/s13762-019-02215-8. http://link.springer.com/10.1007/s13762-019-02215-8. Center for Environmental and Energy Research and Studies.
3. Yang Z, Yang F, Liu JL, Wu HT, Yang H, Shi Y, et al. Heavy metal transporters: functional mechanisms, regulation, and application in phytoremediation. Sci Total Environ. 2022. Elsevier B.V.
4. Bothe H, Słomka A. Divergent biology of facultative heavy metal plants. J Plant Physiol. 2017;219:45–61. Available from:https://linkinghub.elsevier.com/retrieve/pii/S0176161717302341.
5. Visioli G, D'Egidio S, Sanangelantoni AM. The bacterial rhizobiome of hyperaccumulators: future perspectives based on omics analysis and advanced microscopy. Front Plant Sci. 2015;5. Available from: http://journal.frontiersin.org/article/10.3389/fpls.2014.00752/abstract.
6. Thijs S, Langill T, Vangronsveld J. The bacterial and fungal microbiota of hyperaccumulator plants. 2017. p. 43–86. Available from: https://linkinghub.elsevier.com/retrieve/pii/S0065229616301227.
7. Alford ÉR, Pilon-Smits EAH, Paschke MW. Metallophytes-a view from the rhizosphere. Plant Soil. 2010;337:33–50.
8. Mathivanan K, Chandirika JU, Vinothkanna A, Yin H, Liu X, Meng D. Bacterial adaptive strategies to cope with metal toxicity in the contaminated environment – a review. Ecotoxicol Environ Saf: Academic Press; 2021.

9. Priyadarshini E, Priyadarshini SS, Cousins BG, Pradhan N. Metal-Fungus interaction: review on cellular processes underlying heavy metal detoxification and synthesis of metal nanoparticles. Chemosphere. 2021;274:129976. https://doi.org/10.1016/j.chemosphere.2021.129976. https://linkinghub.elsevier.com/retrieve/pii/S0045653521004458. Elsevier Ltd.
10. da Silva LJ, de Rezende Pinto F, do Amaral LA, Garcia-Cruz CH. Biosorption of cadmium (II) and lead (II) from aqueous solution using exopolysaccharide and biomass produced by Colletotrichum sp. Desalination Water Treat. 2014;52:7878–86.
11. Diego Valenzuela-Cobos J, Grijalva A, Marcillo R, Garcés F. Production of exopolysaccharides of Colletotrichum gloeosporioides and Rhizopus stolonifer to absorb lead in the sediment of aquaculture pool. 2020. Available from: www.ejabf.journals.ekb.eg.
12. Singh SK, Wu X, Shao C, Zhang H. Microbial enhancement of plant nutrient acquisition. Stress Biol. 2022;2(1):3 https://link.springer.com/10.1007/s44154-021-00027-w. Springer.
13. Flores-Gallegos AC, Nava-Reyna E. Plant growth-promoting microbial enzymes. In: Enzymes in food biotechnology: production, applications, and future prospects. Elsevier Inc.; 2018. Available from: https://doi.org/10.1016/B978-0-12-813280-7.00030-X.
14. Wang Y, Narayanan M, Shi X, Chen X, Li Z, Natarajan D, et al. Plant growth-promoting bacteria in metal-contaminated soil: current perspectives on remediation mechanisms. Front Microbiol. 2022;13:966226 Frontiers Media S.A.
15. Henagamage AP, Peries CM, Seneviratne G. Fungal-bacterial biofilm mediated heavy metal rhizo-remediation. World J Microbiol Biotechnol. 2022;38:85. Available from:https://link.springer.com/10.1007/s11274-022-03267-8.
16. Liu X, Mei S, Salles JF. Inoculated microbial consortia perform better than single strains in living soil: a meta-analysis. Applied Soil Ecology. 2023;190:105011.
17. Durand A, Gonnelli C, Lopez S, Coppi A, Bacci G, Benizri E. Plant genetics and site properties influenced the diversity of seed endophytic bacterial communities of Odontarrhena species from serpentine soil of Albania. Plant Soil. 2022;481:427–46.
18. Durand A, Leglize P, Lopez S, Sterckeman T, Benizri E. Noccaea caerulescens seed endosphere: a habitat for an endophytic bacterial community preserved through generations and protected from soil influence. Plant Soil. 2022;472:257–78.
19. Ancousture J, Durand A, Blaudez D, Benizri E. A reduced but stable core microbiome found in seeds of hyperaccumulators. Science of the Total Environment. 2023;887.
20. Jaffré T, Pillon Y, Thomine S, Merlot S. The metal hyperaccumulators from New Caledonia can broaden our understanding of nickel accumulation in plants. Front Plant Sci. 2013;4:279.
21. Gei V, Isnard S, Erskine PD, Echevarria G, Fogliani B, Jaffré T, et al. A systematic assessment of the occurrence of trace element hyperaccumulation in the flora of New Caledonia. Bot J Linnean Soc. 2020;XX:1–22. Available from: https://academic.oup.com/botlinnean/article-abstract/doi/10.1093/botlinnean/boaa029/5874218.
22. Callahan DL, Roessner U, Dumontet V, De Livera AM, Doronila A, Baker AJM, et al. Elemental and metabolite profiling of nickel hyperaccumulators from New Caledonia. Phytochemistry. 2012;81:80–9.
23. González DA, de la Torre VSG, Fernández RR, Barreau L, Merlot S. Divergent roles of IREG/Ferroportin transporters from the nickel hyperaccumulator Leucocroton havanensis. Physiol Plant. 2024;176:e14261.
24. García de la Torre VS, Majorel-Loulergue C, Rigaill GJ, Alfonso-González D, Soubigou-Taconnat L, Pillon Y, et al. Wide cross-species RNA-seq comparison reveals convergent molecular mechanisms involved in nickel hyperaccumulation across dicotyledons. New Phytologist. 2021;229:994–1006.
25. Jaffré T, Schmid M. Accumulation du nickel par une Rubiacée de Nouvelle-Calédonie, Psychotria douarrei (G. Beauvisage) Däniker. Comptes Rendus de l'Académie des Sciences de Paris, Série D. 1974;278:1727–30.
26. Gonin M, Gensous S, Lagrange A, Ducousso M, Amir H, Jourand P. Rhizosphere bacteria of Costularia spp. from ultramafic soils in New Caledonia: diversity, tolerance to extreme edaphic conditions, and role in plant growth and mineral nutrition. Can J Microbiol. 2013;59:164–74.
27. Bourles A, Guentas L, Chalkiadakis E, Majorel C, Juillot F, Cavaloc Y, et al. New caledonian ultramafic conditions structure the features of curtobacterium citreum strains that play a role in plant adaptation. Can J Microbiol. 2019;65:880–94.
28. Bourles A, Guentas L, Charvis C, Gensous S, Majorel C, Crossay T, et al. Co-inoculation with a bacterium and arbuscular mycorrhizal fungi improves root colonization, plant mineral nutrition, and plant growth of a Cyperaceae plant in an ultramafic soil. Mycorrhiza. 2020;30:121–31.
29. Wickham H. ggplot2: elegant graphics for data analysis. Springer-Verlag New York; 2016. Available from: https://ggplot2.tidyverse.org.
30. Cheng J, Schloerke B, Karambelkar B, Xie Y. leaflet: create interactive web maps with the JavaScript 'Leaflet' Library. 2024. Available from: https://CRAN.R-project.org/package=leaflet.
31. Mosse B. The establishment of vesicular-arbuscular mycorrhiza under aseptic conditions. J Gen Microbiol. 1962;27:509–20.
32. Daniels BA, Menge JA. Evaluation of the commercial potential of the vesicular-arbuscular mycorrhizal fungus, Glomus epigaeus. New Phytol. 1981;87:345–54.
33. Villegente M. Caractérisation Biochimique et Moléculaire de Mécanismes de la Germination d'Espèces Endémiques de Nouvelle-Calédonie [Thèse de doctorat]. [Nouméa, Nouvelle-Calédonie]: Université de la Nouvelle-Calédonie; 2013. Available from: https://tel.archives-ouvertes.fr/tel-02967465.
34. Gourmelon V, Maggia L, Powell JR, Gigante S, Hortal S, Gueunier C, et al. Environmental and geographical factors structure soil microbial diversity in new caledonian ultramafic substrates: a metagenomic approach. PLoS One. 2016;11:1–25. https://doi.org/10.1371/journal.pone.0167405.
35. Salzman RA, Fujita T, Zhu-Salzman K, Hasegawa PM, Bressan RA. An improved RNA isolation method for plant tissues containing high levels of phenolic compounds or carbohydrates. Plant Mol Biol Report. 1999;17(1):11–7. https://doi.org/10.1023/A:1007520314478.
36. Herlemann DPR, Labrenz M, Jürgens K, Bertilsson S, Waniek JJ, Andersson AF. Transitions in bacterial communities along the 2000 km salinity gradient of the Baltic Sea. ISME J. 2011;5:1571–9.
37. White TJ, Bruns TD, Lee SB, Taylor JW. Amplification and direct sequencing of fungal ribosomal RNA genes for phylogenetics. In: Innis MA, Gelfand DH, Sninsky JJ, White TJ, editors. PCR protocols: a guide to methods and applications. New York: Academic Press; 1990. p. 315–22.
38. Andrews S, Krueger F, Segonds-Pichon A, Biggins L, Krueger C, Wingett S. FastQC. UK: Babraham; 2012.
39. Ewels P, Magnusson M, Lundin S, Käller M. MultiQC: summarize analysis results for multiple tools and samples in a single report. Bioinformatics. 2016;32:3047–8. Available from:https://academic.oup.com/bioinformatics/article/32/19/3047/2196507.
40. Van Rossum G, Drake Jr FL. Python reference manual. Centrum voor Wiskunde en Informatica Amsterdam; 1995.
41. Martin M. Cutadapt removes adapter sequences from high-throughput sequencing reads. EMBnet J. 2011;17:10. Available from:http://journal.embnet.org/index.php/embnetjournal/article/view/200.
42. Callahan B. DADA2: project documentation. 2024.
43. Callahan BJ, McMurdie PJ, Rosen MJ, Han AW, Johnson AJA, Holmes SP. DADA2: high-resolution sample inference from Illumina amplicon data. Nat Methods. 2016;13:581–3. Available from:https://www.nature.com/articles/nmeth.3869.
44. McLaren MR, Callahan BJ. Silva 138.1 prokaryotic SSU taxonomic training data formatted for DADA2. Zenodo; 2021. https://doi.org/10.5281/zenodo.4587955.
45. Abarenkov K, Zirk A, Piirmann T, Pöhönen R, Ivanov F, Nilsson RH, et al. UNITE general FASTA release for eukaryotes. UNITE Community. 2022. https://doi.org/10.15156/BIO/2938070.
46. Liu C, Cui Y, Li X, Yao M. microeco : an R package for data mining in microbial community ecology. FEMS Microbiol Ecol. 2021;97:fiaa255. Available from:https://academic.oup.com/femsec/article/doi/10.1093/femsec/fiaa255/6041020.
47. R Core Team. R: a language and environment for statistical computing. Vienna; 2022. Available from: https://www.R-project.org/.
48. RStudio Team. RStudio: integrated development environment for R. Boston; 2020. Available from: http://www.rstudio.com/.
49. Oksanen J, Simpson GL, Blanchet FG, Kindt R, Legendre P, Minchin PR, et al. vegan: Community Ecology Package. 2022. Available from: https://CRAN.R-project.org/package=vegan.

50. Mangiafico SS. rcompanion: functions to support extension education program evaluation. New Brunswick, New Jersey; 2024. Available from: https://CRAN.R-project.org/package=rcompanion/.
51. Wolda H. Similarity indices, sample size and diversity. Oecologia. 1981;50:296–302.
52. Dusa A. venn: Draw Venn Diagrams. 2024. Available from: https://CRAN.R-project.org/package=venn.
53. Inkscape Developers. Inkscape. 2022. Available from: https://inkscape.org.
54. Revelle W. psych: procedures for psychological, psychometric, and personality research. Evanston, Illinois; 2024. Available from: https://CRAN.R-project.org/package=psych.
55. Csárdi G, Nepusz T, Traag V, Horvát S, Zanini F, Noom D, et al. igraph: Network analysis and visualization in R. 2024. Available from: https://cran.r-project.org/package=igraph.
56. Yuan MM, Guo X, Wu L, Zhang Y, Xiao N, Ning D, et al. Climate warming enhances microbial network complexity and stability. Nat Clim Chang. 2021;11:343–8.
57. Banerjee S, Schlaeppi K, van der Heijden MGA. Keystone taxa as drivers of microbiome structure and functioning. Nat Rev Microbiol. 2018;16:567–76.
58. Trivedi P, Leach JE, Tringe SG, Sa T, Singh BK. Plant–microbiome interactions: from community assembly to plant health. Nat Rev Microbiol. 2020;18:607–21. Available from:https://www.nature.com/articles/s41579-020-0412-1.
59. Ren W, Zhong Y, Ding Y, Wu Y, Xu X, Zhou P. Mismatches in 16S rRNA gene primers: an area worth further exploring. Front Microbiol. 2022;13:13.
60. Thomas F, Dittami SM, Brunet M, Le Duff N, Tanguy G, Leblanc C, et al. Evaluation of a new primer combination to minimize plastid contamination in 16S rDNA metabarcoding analyses of alga-associated bacterial communities. Environ Microbiol Rep. 2020;12:30–7.
61. Gei V, Echevarria G, Erskine PD, Isnard S, Fogliani B, Montargès-Pelletier E, et al. Soil chemistry, elemental profiles and elemental distribution in nickel hyperaccumulator species from New Caledonia. Plant Soil. 2020;457:293–320. Available from:https://link.springer.com/10.1007/s11104-020-04714-x.
62. Kwak MJ, Jeong H, Madhaiyan M, Lee Y, Sa TM, Oh TK, et al. Genome information of Methylobacterium oryzae, a plant-probiotic methylotroph in the phyllosphere. PLoS One. 2014;9:e106704.
63. Madhaiyan M, Poonguzhali S, Sa T. Metal tolerating methylotrophic bacteria reduces nickel and cadmium toxicity and promotes plant growth of tomato (Lycopersicon esculentum L.). Chemosphere. 2007;69:220–8.
64. Dourado MN, Camargo Neves AA, Santos DS, Araújo WL. Biotechnological and agronomic potential of endophytic pink-pigmented methylotrophic methylobacterium spp. Biomed Res Int. 2015;2015:1–19 http://www.hindawi.com/journals/bmri/2015/909016/. Hindawi Publishing Corporation.
65. Chen J, Li N, Han S, Sun Y, Wang L, Qu Z, et al. Characterization and bioremediation potential of nickel-resistant endophytic bacteria isolated from the wetland plant Tamarix chinensis. FEMS Microbiol Lett. 2020;367:1–7.
66. Fan D, Schwinghamer T, Liu S, Xia O, Ge C, Chen Q, et al. Characterization of endophytic bacteriome diversity and associated beneficial bacteria inhabiting a macrophyte Eichhornia crassipes. Front Plant Sci. 2023;14:1176648.
67. Lee SY, Lee YY, Cho KS. Inoculation effect of heavy metal tolerant and plant growth promoting rhizobacteria for rhizoremediation. Int J Environ Sci Technol. 2024;21:1419–34.
68. Rangel WM, de Oliveira Longatti SM, Ferreira PAA, Bonaldi DS, Guimarães AA, Thijs S, et al. Leguminosae native nodulating bacteria from a gold mine as-contaminated soil: multi-resistance to trace elements, and possible role in plant growth and mineral nutrition. Int J Phytoremediation. 2017;19:925–36.
69. Rathi M, Nandabalan YK. Copper-tolerant rhizosphere bacteria—characterization and assessment of plant growth promoting factors. Environ Sci Pollut Res. 2017;24:9723–33.
70. Rosatto S, Roccotiello E, Di Piazza S, Cecchi G, Greco G, Zotti M, et al. Rhizosphere response to nickel in a facultative hyperaccumulator. Chemosphere. 2019;232:243–53.
71. Stajković-Srbinović O, De Meyer SE, Kuzmanović D, Dinić Z, Delić D, Willems A. Soybean seed chemical composition as influenced by Bradyrhizobium inoculation in soils with elevated nickel concentrations. Appl Soil Ecol. 2020;153:103576.
72. Wani PA, Khan MS, Zaidi A. Effect of metal tolerant plant growth promoting Bradyrhizobium sp. (vigna) on growth, symbiosis, seed yield and metal uptake by greengram plants. Chemosphere. 2007;70:36–45.
73. Asaf S, Numan M, Khan AL, Al-Harrasi A. Sphingomonas: from diversity and genomics to functional role in environmental remediation and plant growth. Crit Rev Biotechnol. Taylor and Francis Ltd; 2020. p. 138–52.
74. do Espírito Santo BC, Oliveira JA, Ribeiro MA, et al. Antitumor and antibacterial activity of metabolites of endophytic {Colletotrichum} siamense isolated from coffee ({Coffea} arabica L. cv IAPAR-59). Brazilian J Microbiol. 2023;54:2651–61.
75. Peng WW, Kuang M, Huang YT, Li MF, Zheng YT, Xu L, et al. Pseudocercones A-C, three new polyketide derivatives from the endophytic fungus Pseudocercospora sp. TSS-1. Nat Prod Res. 2024;38:1248–55. https://doi.org/10.1080/14786419.2022.2138874.
76. Riga R, Happyana N, Hakim EH. Secondary metabolites from Colletotrichum gloeosporioides isolated from Artocarpus heterophyllus and evaluation of their cytotoxic and antibacterial activities. Nat Prod Res. 2023;0:1–7. https://doi.org/10.1080/14786419.2023.2269596.
77. Thomas LV, Yu S, Ingram RE, Refdahl C, Elsser D, Delves-Broughton J. Ascopyrone P, a novel antibacterial derived from fungi. J Appl Microbiol. 2002;93:697–705.
78. Yang MH, Li TX, Wang Y, Liu RH, Luo J, Kong LY. Antimicrobial metabolites from the plant endophytic fungus Penicillium sp. Fitoterapia. 2017;116:72–6.
79. Zhao WT, Shi X, Xian PJ, Feng Z, Yang J, Yang XL. A new fusicoccane diterpene and a new polyene from the plant endophytic fungus Talaromyces pinophilus and their antimicrobial activities. Nat Prod Res. 2021;35:124–30.
80. Alexander I, Selosse MA. Mycorrhizas in tropical forests: a neglected research imperative. In: New Phytologist. 2009. p. 14–6.
81. Jourand P, Carriconde F, Ducousso M, Majorel C, Hannibal L, Prin Y, et al. Abundance, distribution and function of Pisolithus albus and other ectomycorrhyzal fungi of ultramafic soils in New Caledonia. In: Bâ AA, McGuire KL, Diédhiou AG, editors. Ectomycorrhizal symbioses in tropical and neotropical forests. Boca Raton: CRC Press; 2014. p. 100–25. Available from: https://www.taylorfrancis.com/books/9781466594692/chapters/10.1201/b16536-7.
82. Kier G, Kreft H, Lee TM, Jetz W, Ibisch PL, Nowicki C, et al. A global assessment of endemism and species richness across island and mainland regions. Proc Natl Acad Sci U S A. 2009;106:9322–7.
83. Pillon Y, Jaffré T, Birnbaum P, Bruy D, Cluzel D, Ducousso M, et al. REVIEW Infertile landscapes on an old oceanic island: the biodiversity hotspot of New Caledonia. Biol J Linnean Soc. 2021. Available from: https://academic.oup.com/biolinnean/article/133/2/317/5957448.
84. Carriconde F, Gardes M, Bellanger JM, Letellier K, Gigante S, Gourmelon V, et al. Host effects in high ectomycorrhizal diversity tropical rainforests on ultramafic soils in New Caledonia. Fungal Ecol. 2019;39:201–12.
85. Lopez S, Goux X, Echevarria G, Calusinska M, Morel JL, Benizri E. Community diversity and potential functions of rhizosphere-associated bacteria of nickel hyperaccumulators found in Albania. Sci Total Environ. 2019;654:237–49.
86. Durand A, Maillard F, Alvarez-Lopez V, Guinchard S, Bertheau C, Valot B, et al. Bacterial diversity associated with poplar trees grown on a Hg-contaminated site: community characterization and isolation of Hg-resistant plant growth-promoting bacteria. Sci Total Environ. 2018;622–623:1165–77.
87. Durand A, Goux X, Lopez S, Leglize P, Benizri E. Soil nickel contamination levels entail changes in the bacterial communities associated to the rhizosphere and endosphere of Odontarrhena chalcidica. Plant Soil. 2023;493:17–43.
88. Jiang Y, Luo J, Guo X, Qiao Y, Li Y, Zhang Y, et al. Phyllosphere microbiome assists the hyperaccumulating plant in resisting heavy metal stress. J Environ Sci. 2024;154:563–74. https://doi.org/10.1016/j.jes.2024.05.032. https://linkinghub.elsevier.com/retrieve/pii/S1001074224002717. Elsevier BV.

89. Toghueo RMK, Zabalgogeazcoa I, Pereira EC, Vazquez de Aldana BR. A diaporthe fungal endophyte from a wild grass improves growth and salinity tolerance of tritordeum and perennial ryegrass. Front Plant Sci. 2022;13:896755.
90. Chen L, Kang W, Shen M, Tao H, Wang C, Zheng J, et al. Adaptation of rhizosphere and endosphere microbiome to heavy metal pollution in castor bean. Rhizosphere. 2022;24:24.
91. Zhang X, Chen B, Yin R, Xing S, Fu W, Wu H, et al. Long-term nickel contamination increased soil fungal diversity and altered fungal community structure and co-occurrence patterns in agricultural soils. J Hazard Mater. 2022;436:129113.
92. Sharma VK, Li XY, Wu GL, Bai WX, Parmar S, White JF, et al. Endophytic community of Pb-Zn hyperaccumulator Arabis alpina and its role in host plants metal tolerance. Plant Soil. 2019;437:397–411.
93. Zhu M, Ding Y, Li X, Xiao Y, Zhao Z, Li T. Biodiversity of root endophytic fungi from oxyria sinensis grown in metal-polluted and unpolluted soils in yunnan province, southwestern china. Plants. 2021;10:10.
94. Mao W, Wu Y, Li Q, Xiang Y, Tang W, Hu H, et al. Seed endophytes and rhizosphere microbiome of Imperata cylindrica, a pioneer plant of abandoned mine lands. Front Microbiol. 2024;15:15.
95. Wu Y, Ma L, Zhang X, Topalović O, Liu Q, Feng Y, et al. A hyperaccumulator plant Sedum alfredii recruits Cd/Zn-tolerant but not Pb-tolerant endospheric bacterial communities from its rhizospheric soil. Plant Soil. 2020;455:257–70.
96. Zarraonaindia I, Owens SM, Weisenhorn P, West K, Hampton-Marcell J, Lax S, et al. The soil microbiome influences grapevine-associated microbiota. mBio. 2015;6:10–128.
97. Ważny R, Rozpądek P, Domka A, Jędrzejczyk RJ, Nosek M, Hubalewska-Mazgaj M, et al. The effect of endophytic fungi on growth and nickel accumulation in Noccaea hyperaccumulators. Sci Total Environ. 2021;768: 144666.
98. Lankinen P, Kähkönen MA, Rajasärkkä J, Virta M, Hatakka A. The effect of nickel contamination on the growth of litter-decomposing fungi, extracellular enzyme activities and toxicity in soil. Boreal Environ Res. 2011;16:229–39.
99. Idris R, Trifonova R, Puschenreiter M, Wenzel WW, Sessitsch A. Bacterial communities associated with flowering plants of the Ni hyperaccumulator Thlaspi goesingense. Appl Environ Microbiol. 2004;70:2667–77.
100. Mukherjee D, Pramanik K, Mandal S, Mandal NC. Augmented growth of Cd-stressed rice seedlings with the application of phytostimulating, root-colonizing, Cd-tolerant, leaf-endophytic fungi Colletotrichum spp. isolated from Eupatorium triplinerve. J Hazard Mater. 2022;438:438.
101. Roy S, Mukherjee B, Dutta S. Isolation of an endophytic fungus Colletotrichum sp. and study of its plant growth promoting traits. Pharma Innov. 2021;10:1038–44.
102. Dell'Amico E, Cavalca L, Andreoni V. Analysis of rhizobacterial communities in perennial Graminaceae from polluted water meadow soil, and screening of metal-resistant, potentially plant growth-promoting bacteria. FEMS Microbiol Ecol. 2005;52:153–62.
103. Cecchi G, Roccotiello E, Di Piazza S, Riggi A, Mariotti MG, Zotti M. Assessment of Ni accumulation capability by fungi for a possible approach to remove metals from soils and waters. J Environ Sci Health B. 2017;52:166–70.
104. Mondal P, Datta B, Chaudhuri S. A highly heavy metal tolerant Fusarium solani with efficient bioaccumulation potentiality from contaminated soil. Journal of Experimental Biology and Agricultural Sciences. 2019;7:579–86.
105. Mohammed YMM, Khedr YI. Applications of Fusarium solani YMM20 in bioremediation of heavy metals via enhancing extracellular green synthesis of nanoparticles. Water Environ Res. 2021;93:1600–7.
106. Hassan A, Pariatamby A, Ossai IC, Ahmed A, Muda MA, Barasarathi J, et al. Synergistic association of endophytic fungi enhances tolerance, growth, and heavy metal uptake of Alocasia calidora in landfill contaminated soil. Applied Soil Ecology. 2022;170:104307.
107. Sharma R, Jasrotia T, Kumar R, Kumar R, Alothman AA, AL-Anazy MM, et al. Multi-biological combined system: a mechanistic approach for removal of multiple heavy metals. Chemosphere. 2021;276:130018.
108. Montaser DA, Easa SM, A Mansour MM, Mohamed SS. The efficiency of some locally isolated fungi on removing Pb, Cd, Cr and Ni and their mixture from wastewater e-mail. Egypt J Pure Appl Sci. 2022.
109. El-Shahir AA, El-Tayeh NA, Ali OM, Abdel Latef AAH, Loutfy N. The effect of endophytic Talaromyces pinophilus on growth, absorption and accumulation of heavy metals of Triticum aestivum grown on sandy soil amended by Sewage Sludge. Plants. 2021;10(12):2659.
110. Rossiana N, Joko K, Yayat D. Utilization of Talaromyces sp., Cladosporium sp. and Albizia (Paraserianthes falcataria L. Nielsen) Mycorrhizae on the Phytoremediation of oil sludge: changes of lead, nickel, total petroleum hydrocarbon (TPH) and polycyclic aromatic hydrocarbons (PAH) contents. J Pet Environ Biotechnol. 2018;09:1755.
111. Abou-Shanab RAI, van Berkum P, Angle JS. Heavy metal resistance and genotypic analysis of metal resistance genes in gram-positive and gram-negative bacteria present in Ni-rich serpentine soil and in the rhizosphere of Alyssum murale. Chemosphere. 2007;68:360–7.
112. Schmidt A, Hagen M, Schütze E, Schmidt A, Kothe E. In silico prediction of potential metallothioneins and metallohistins in actinobacteria. J Basic Microbiol. 2010;50:562–9.
113. Hu X, Liu X, Qiao L, Zhang S, Su K, Qiu Z, et al. Study on the spatial distribution of ureolytic microorganisms in farmland soil around tailings with different heavy metal pollution. Science of the Total Environment. 2021;775:144946.
114. Babu AG, Shim J, Bang KS, Shea PJ, Oh BT. Trichoderma virens PDR-28: A heavy metal-tolerant and plant growth-promoting fungus for remediation and bioenergy crop production on mine tailing soil. J Environ Manage. 2014;132:129–34.
115. Syed A, Elgorban AM, Bahkali AH, Eswaramoorthy R, Iqbal RK, Danish S. Metal-tolerant and siderophore producing Pseudomonas fluorescence and Trichoderma spp. improved the growth, biochemical features and yield attributes of chickpea by lowering Cd uptake. Sci Rep. 2023;13:13.
116. Cao L, Jiang M, Zeng Z, Du A, Tan H, Liu Y. Trichoderma atroviride F6 improves phytoextraction efficiency of mustard (Brassica juncea (L.) Coss. var. foliosa Bailey) in Cd, Ni contaminated soils. Chemosphere. 2008;71:1769–73.
117. Hanley ML, Vukicevich E, Rice AM, Richardson JB. Uptake of toxic and nutrient elements by foraged edible and medicinal mushrooms (sporocarps) throughout Connecticut River Valley, New England, USA. Environ Sci Pollut Res Int. 2024;31:5526–39.
118. Singh RP, Shelke GM, Kumar A, Jha PN. Biochemistry and genetics of ACC deaminase: a weapon to 'stress ethylene' produced in plants. Front Microbiol. 2015. Frontiers Media S.A.
119. Arteca RN, Arteca JM. Heavy-metal-induced ethylene production in Arabidopsis thaliana. J Plant Physiol. 2007;164(11):1480–8. https://doi.org/10.1016/j.jplph.2006.09.006.
120. Iqbal N, Khan NA, Ferrante A, Trivellini A, Francini A, Khan MIR. Ethylene role in plant growth, development and senescence: interaction with other phytohormones. Front Plant Sci. 2017;8:475.
121. Hummel W. The influence of cyanide complexation on the speciation and solubility of radionuclides in a geological repository. Environ Geol. 2004;45:633–46.
122. Gupta P, Diwan B. Bacterial Exopolysaccharide mediated heavy metal removal: a review on biosynthesis, mechanism and remediation strategies. Biotechnol Rep. 2017;13:58–71 Elsevier B.V.
123. Gomes AFR, Almeida MC, Sousa E, Resende DISP. Siderophores and metallophores: metal complexation weapons to fight environmental pollution. Sci Total Environ. 2024;932:173044. Available from:https://www.sciencedirect.com/science/article/pii/S0048969724031917.
124. Likar M, Regvar M. Isolates of dark septate endophytes reduce metal uptake and improve physiology of Salix caprea L. Plant Soil. 2013;370:593–604.
125. Xiao Y, Chen R, Chen L, Yang B, Jiang L, Fang J. Endophytic fungus Talaromyces sp. MR1 promotes the growth and cadmium uptake of Arabidopsis thaliana L. under cadmium stress. Curr Microbiol. 2023;80:80.
126. Sun J, Zou X, Xiao T, Jia Y, Ning Z, Sun M, et al. Biosorption and bioaccumulation of thallium by thallium-tolerant fungal isolates. Environ Sci Pollut Res. 2015;22:16742–8.
127. Dell'Amico E, Cavalca L, Andreoni V. Improvement of Brassica napus growth under cadmium stress by cadmium-resistant rhizobacteria. Soil Biol Biochem. 2008;40:74–84.
128. Jin W, Peng L, Zhang X, Sun H, Yuan Z. Effects of endophytic and ectomycorrhizal basidiomycetes on Quercus virginiana seedling growth and nutrient absorption. J Sustain For. 2019;38:457–70.

129. Peng L, Shan X, Yang Y, Wang Y, Druzhinina IS, Pan X, et al. Facultative symbiosis with a saprotrophic soil fungus promotes potassium uptake in American sweetgum trees. Plant Cell Environ. 2021;44:2793–809.
130. Zhang H, Zhou H, Bai J, Li Y, Yang J, Ma Q, et al. Biosynthesis of selenium nanoparticles mediated by fungus Mariannaea sp. HJ and their characterization. Colloids Surf A Physicochem Eng Asp. 2019;571:9–16.
131. Samynathan R, Venkidasamy B, Ramya K, Muthuramalingam P, Shin H, Kumari PS, et al. A recent update on the impact of nano-selenium on plant growth, metabolism, and stress tolerance. Plants. 2023;12: 853.
132. Syed A, Elgorban AM, Bahkali AH, Eswaramoorthy R, Iqbal RK, Danish S. Metal-tolerant and siderophore producing Pseudomonas fluorescence and Trichoderma spp. improved the growth, biochemical features and yield attributes of chickpea by lowering Cd uptake. Sci Rep. 2023;13:4471.
133. Hu X, Liu X, Qiao L, Zhang S, Su K, Qiu Z, et al. Study on the spatial distribution of ureolytic microorganisms in farmland soil around tailings with different heavy metal pollution. Sci Total Environ. 2021;775: 144946.
134. Abanda-Nkpwatt D, Musch M, Tschiersch J, Boettner M, Schwab W. Molecular interaction between Methylobacterium extorquens and seedlings: growth promotion, methanol consumption, and localization of the methanol emission site. J Exp Bot. 2006;57:4025–32.
135. Dourado MN, Ferreira A, Araújo WL, Azevedo JL, Lacava PT. The diversity of endophytic methylotrophic bacteria in an oil-contaminated and an oil-free mangrove ecosystem and their tolerance to heavy metals. Biotechnol Res Int. 2012;2012:1–8.
136. Fernandes VC, Albergaria JT, Oliva-Teles T, Delerue-Matos C, De Marco P. Dual augmentation for aerobic bioremediation of MTBE and TCE pollution in heavy metal-contaminated soil. Biodegradation. 2009;20:375–82.

Publisher's Note